United States
Department of
Agriculture

Forest Service

**Southern
Research Station**

General Technical
Report SO-125

Techniques in Experimental Mechanics Applicable to Forest Products Research

Proceedings of the Experimental Mechanics Plenary Session at the Forest Products Research Society Annual Meeting

Portland, ME — June 29, 1994

April 1998

Southern Research Station
P.O. Box 2680
Asheville, North Carolina 28802

Techniques in Experimental Mechanics Applicable to Forest Products Research

Proceedings of the Experimental Mechanics Plenary Session at the Forest Products Research Society Annual Meeting

Portland, ME
June 29, 1994

Editors

Leslie H. Groom and Audrey G. Zink
USDA Forest Service, Southern Forest Experiment Station,
Pineville, LA

Conducted by

USDA Forest Service, Virginia Polytechnic Institute
and State University, and the Forest Products Society,
Blacksburg, VA

Contents

Introduction to Techniques in Experimental Mechanics

Leslie H. Groom and Audrey G. Zink

The title of this publication-Techniques *in Experimental Mechanics Applicable to Forest Products Research-is* the theme of this plenary session from the 1994 Annual Meeting of the Forest Products Society (FPS). Although this session focused on experimental techniques that can be of assistance to researchers in the field of forest products, it is hoped that the techniques and findings presented are beneficial to the forest products industry as well. The presentations given during the plenary session ranged from short-term, applied research to long-term, fundamental research. Both types of research are necessary for the health and productivity of the forest products industry; applied research provides information that can be immediately implemented to improve product performance, yield, and/or reliability, while fundamental research is instrumental in product development and global competitiveness.

Research has long been at the heart of any type of industry that relies on engineered products. This has been the case with the forest products industry. There have been many changes in technology over the past several years, due primarily to the rapid advancements in digital processing. One of the results from these advancements is a new generation of instruments and algorithms that rely on the collection and analysis of vast amounts of data, thus allowing researchers to obtain information on stresses and strains in wood and wood-based composites in manners previously unattainable. Although it was impossible to adequately cover all of the recent advancements in equipment and techniques, the main objective of this session was to present an overview of new categories of equipment, how this equipment is used, what type of results can be achieved, and where the research is being conducted. Articles within this report are a compilation of the plenary session presentations. Speakers and contributors were selected on the basis of their knowledge of the subject matter and respect given to them among their colleagues.

Due to the wide range of topics covered by the session, the chairpersons determined that the session would best be introduced with an overview of traditional strain measurement. This overview, given by Joe Loferski, focused on the available types of traditional strain-measuring devices, the limitations associated with each type, and attachment considerations. Joe gave many examples of strain-measurement devices but concentrated primarily on extensometers, clip-on electrical transducers, electrical resistance strain gauges, and tell-tale gauges. Although traditional strain-measurement devices are generally inexpensive and readily available, they rely on contact with the substrate under investigation.

An introduction into noncontact, full-field strain measurement was the focus of the next three presentations. Audrey Zink began the discussion of full-field strain measurement with an introduction to digital image correlation. Equipment and software necessary to produce full-field strain maps were discussed. Although her discussion focused on macrostrains of solid lumber, the methods and techniques are applicable to all levels of scale. This was elaborated upon by the third speaker, Laurence Mott. His talk centered primarily on the development of full-field strain maps of specimens in an environmental scanning electron microscope. Laurence covered a wide variety of topics such as conventional light microscopy, scanning electron microscopy (SEM), environmental SEM, digital image processing, and image acquisition. He also discussed converting traditional load-elongation traces to stress-strain curves by three-dimensional reconstruction algorithms and confocal laser scanning microscopy. Full-field strain analysis was the topic of the fourth speaker, Ron Wolfe. Ron used a completely different approach from the previous two speakers by measuring strains in a metal plate connector by attaching a moire grid and digitally capturing deformations within the grid. He also discussed full-field stress analysis using stress pattern analysis (by measurement of) thermal emissions, commonly referred to as SPATE'.

Leslie H. Groom is a research technologist, USDA Forest Service, Southern Research Station, 2500 Shreveport Hwy., Pineville, LA 71360; Audrey G. Zink is an assistant professor, Department of Wood Science and Forest Products, Virginia Polytechnic Institute and State University, Blacksburg. VA 24061-0323.

This type of analysis indirectly measures stresses by monitoring minute changes in the temperature of the metal plate connector under strain. Although SPATE shows much promise, it should be noted that the apparatus is expensive and that the technique may not be applicable to wood due to the inherent low level of thermal emissions in wood.

The final speaker, Mike Wolcott, focused his presentation not so much on material properties of components within a composite, but rather on the interface between these components. He discussed advantages and limitations of the following micro-mechanical methods commonly used to measure interfacial properties: the fragmentation test, the micro-debond test, the fiber pull-out test, and dynamic mechanical analysis. In addition to the discussion of the techniques, he also presented results discussing the quality of various fiber/matrix interfaces.

A handout outlining the presentations in the session was available during the plenary session, but the supply was not adequate to handle the large audience that attended. Thus, the handout has been provided here in the form of an Appendix. These tables summarize the techniques and methods respectively discussed by all speakers during this session. The tables list equipment discussed, relative cost of the equipment, advantages and limitations of techniques, and some possible applications. It should be noted that the session was represented by industry and research. It is hoped that this session provided useful information for attendees, gave direction as to research tools, and generated discussions that further forest products research and the forest products industry.

Strain Measurement on Wood Using Extensometers, Clip-on Electrical Transducers, Electrical Resistance Strain Gauges, and Tell-Tale Gauges

Joseph R. Loferski

Abstract

Laboratory and field experiments in wood engineering often rely on different types of devices to measure strain. Each type has certain limitations and characteristics that generally dictate its applicability to wood. Some of the issues related to using traditional strain measurement devices on wood and wood-based materials are discussed in this paper.

Introduction

Strain measurements in wood are used for verifying analytical models of wood structures that monitor long-term performance, analyze structural components, such as the linger joints in glue-laminated beams, and, in general, study the physical response of wood structural members to their loads.

The objective of this paper is to identify traditional techniques that have been developed for measuring the strain, especially in wood materials. Strain is a fundamental engineering phenomenon that is produced as a response to an applied stress and is defined as the change in length caused by an applied stress divided by the original length.

From basic mechanics, Hooke's Law is the constitutive model that describes the relationship between stress and strain in the linear range:

$$E = \sigma/\in$$

where

E = elastic modulus,
σ = applied stress, and
$\in$ = strain.

Because wood is nonhomogeneous, hygroscopic, and anisotropic and has anatomical variability, attention to many details is required to produce quality strain measurements, which often is not necessary on isotropic, homogeneous materials. Furthermore, because wood is an electrical and thermal insulator, attention must be directed to heat dissipation when using some strain-measurement devices.

A variety of strain-measuring devices is available to researchers in wood mechanics and wood engineering for use with wood and wood-based materials. The devices include extensometers, clip-on electrical transducers (CET's), electrical resistant strain (ERS) gauges, tell-tale gauges, and full-field strain measuring systems.

The first four methods for measuring strain on wood are described here. Techniques for producing full-field strain measurements are presented elsewhere in these proceedings.

Extensometers

Extensometers are devices that measure the distance between two points on the surface of the object being examined. They include dial gauges, linear variable differential transducers (LVDT's), and other similar devices. The advantages of extensometers are that they are reusable and they can provide fairly long gauge lengths so that the average strain over a representative region of a test specimen can be measured. Disadvantages of extensometers are that many times they are large, heavy, and difficult to attach to the specimen. Furthermore, the thermal expansion of the materials used to construct the extensometer can affect the strain measurements due to temperature changes between measurements.

Figure 1 shows an extensometer consisting of an aluminum bar with a conical point fixed to one end and a dial gauge fixed to the other end. The plunger of the dial gauge is fitted with another conical point. In use, the two conical points are inserted into small metal tubes that are driven into the surface of the specimen. The two tubes provide exact locations at which subsequent readings can be taken.

By using an extensometer, gauge lengths of greater than 50 cm have been successfully produced (Lang 1993). The accuracy of this device is related to the resolution and accuracy of the dial gauge. Recently, digital dial gauges

Joseph R. Loferski is an associate professor, Department of Wood Science and Forest Products, Virginia Polytechnic Institute and State University, Blacksburg, VA 24061-0503.

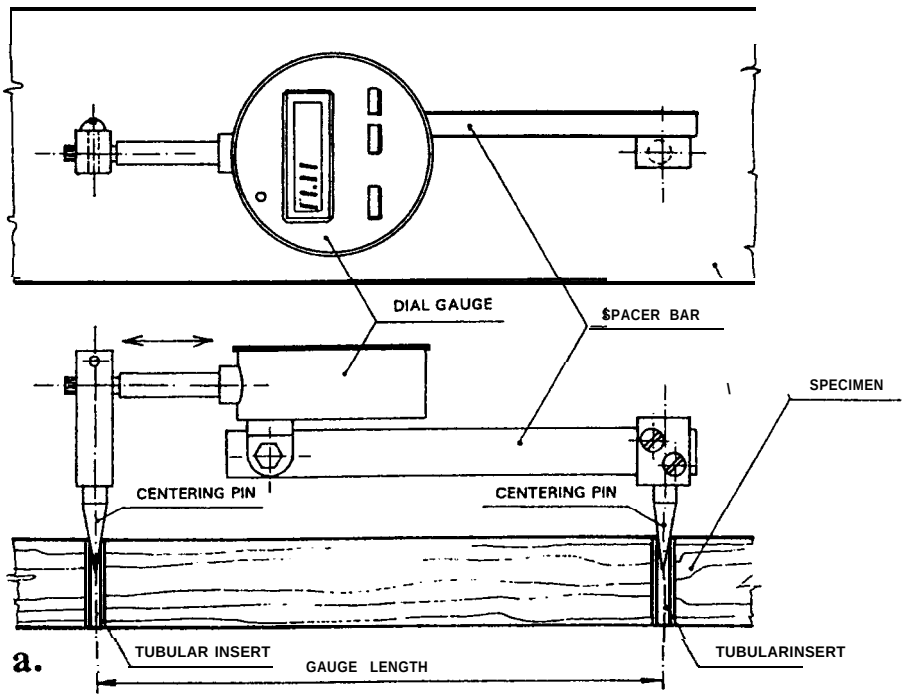

Figure 1—Extensometer showing top and side views (from Lang 1993)

with resolutions approaching 1 0^{-4} mm have become available.

Care must be taken when using this device to align the extensometer perpendicular to the surface of the specimen so that repeatable and accurate measurements can be made.

Clip-on Electrical Transducers

The CET is another type of extensometer that has many applications in testing wood materials. Clip-on electrical transducers are strain gauge transducers, which are commercially produced in laboratories, and that when properly fabricated, calibrated, aligned, and attached to the specimen, are accurate and efficient for measuring strain in wood structural members.

Loferski and others (1989) describe the development and construction of CET's for use in testing wood. The device described has an accuracy of ±0.0005 1 mm per each 55.4 mm gauge length. The CET is easily attached to the specimen and is removable and reusable for testing of multiple specimens. It is economical, custom built, and capable of measuring both large and small strains. Figure 2 shows a schematic diagram of the construction and characteristics of a CET bonded to a specimen.

Figure 3 shows an improved mounting system that utilizes "metallic shoes," which are attached to the specimen with screws to allow precise adjustments of the gauge length and alignment of the gauge with the geometric axis of the specimen. Each CET must be calibrated in a micrometer to produce a displacement vs differential voltage relationship. A typical relationship is shown in figure 4.

When in use, the differential voltage in the gauge is measured and used to compute the displacement of the ends of the gauges. These gauges have been successfully used to measure strain in the surfaces of glue-laminated beams, in creep studies both parallel and perpendicular to the grain, and in bending studies of solid wood elements. To verify the performance of the CET's, an experiment was conducted by Loferski and others (1989) in which bonded, electrical, strain gauges were mounted to a specimen and the CET's were mounted directly over the bonded gauges. An excellent correspondence was found showing that the CET and bonded gauges produce similar strain measurements.

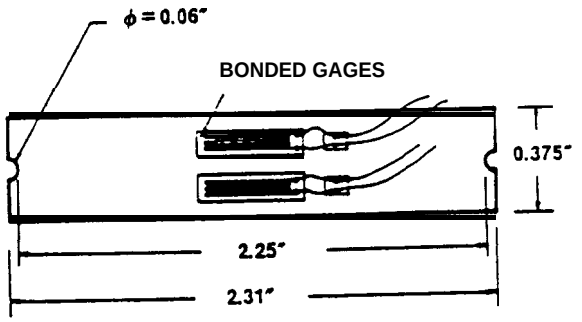

(a) PLAN (WHEN FLAT)

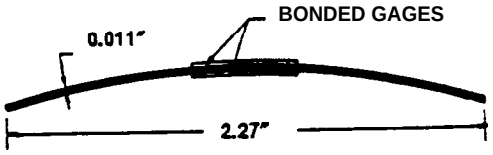

ORIGINAL SHAPE

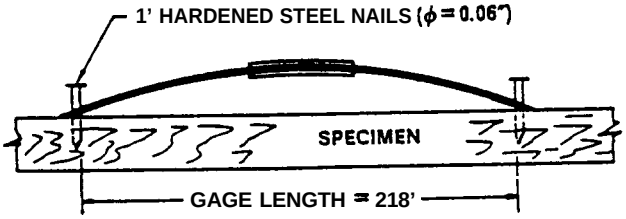

ON TEST-SPECIMEN

(b) ELEVATION

Figure 2—Details of the CET: (a) top and side views showing strain gauges bonded to steel arach; (b) side view showing CET mounted to a wood specimen with two steel nails (from Loferski et al. 1989).

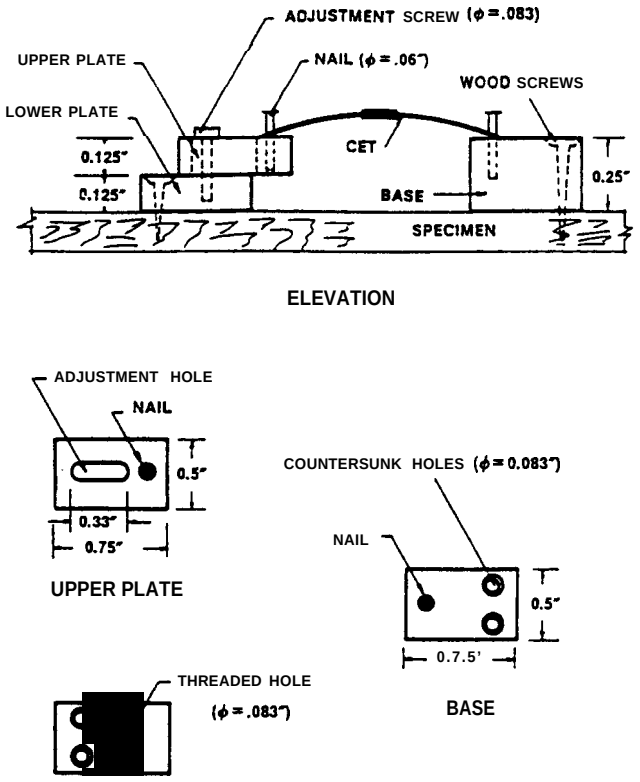

Figure 3-CET mounted to a wood specimen with special adjustable base plates (from Loferski et al. 1989)

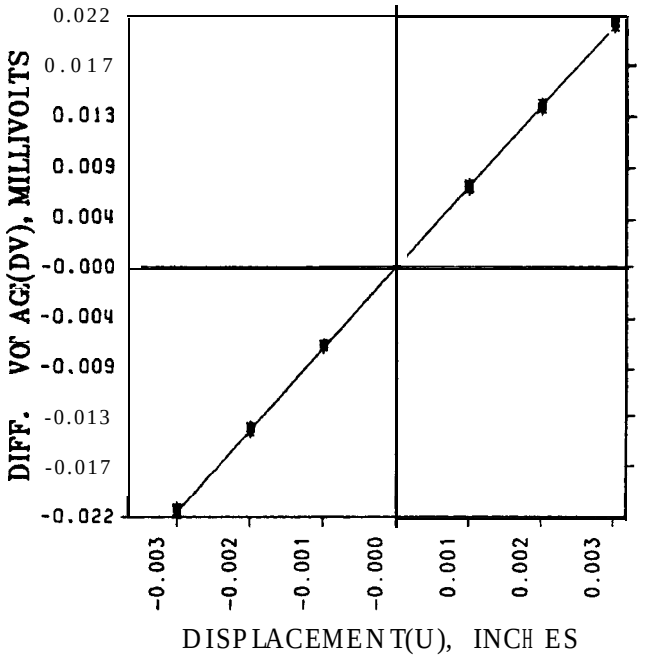

Figure &Typical calibration curve for a CET showing the differential voltage versus the relative displacement of the CET end points (from Loferski et al. 1989)

Commercial extensometers are also available for use in testing materials. Many such devices can be purchased through commercial establishments and can be custom made for specific applications in testing wood materials. Descriptions of these devices are beyond the scope of this paper.

Electrical Resistance Strain Gauges

Electrical resistance strain gauges were invented in 1938 and consist of a strain-sensitive metal in which the electrical'resistance changes in proportion to the strain. Today, ERS gauges are commercially manufactured and consist of a metallic foil mounted in a plastic sheathing. In use, the gauge is bonded with an adhesive to the surface of the specimen. A wheatstone bridge electrical circuit is used to measure the change in the electrical resistance of the gauge. Commercial strain gauges are available in a wide range of sizes and configurations from as small as 0.4 mm to greater than 150 mm gauge lengths.

The ERS gauge has a finite surface area, responds to all strains at all points under its grid, and yields an integrated average strain measurement (Measurements Group 1983). According to Yadama and other (1991), "The measured strain represents the strain at a point from a macromechanics perspective, provided that the strain gauge is not located in a strain gradient and the characteristic length of any material attribute giving rise to inhomogeneity is small relative to the gauge length."

The advantages of ERS gauges include high accuracy, ready commercial availability, and suitability for both long- and short-term measurements. The disadvantages include a relatively high cost and difficulty in mounting and aligning the gauges precisely parallel to the geometric axes of the specimen. In testing wood materials, experiments typically involve many replicates. The fact that the ERS gauges are not reusable from one specimen to the next contributes to the high cost of these types of gauges.

In general, an ideal ERS gauge is small, lightweight, easy to attach to the specimen, has high sensitivity, and is unaffected by temperature, relative humidity, or vibrations. Furthermore, it should be capable of measuring static and dynamic strains, should be inexpensive, and should have an infinitesimal gauge length. However, when considering wood materials, many of these attributes are not applicable. Yadama and others (199 1) state that "the gauge length should be just large enough, but not too large, to record an average macroscopic strain under the gauge, representative of the deformation of the wood specimen around the point of interest." Furthermore, because wood materials are affected by relative humidity and moisture content, which produce swelling of the surface of the material, gauged insulations are affected by changes in temperature or relative humidity.

When selecting an ERS gauge for use on wood, the researcher has many options to consider, including the grid pattern and orientation, the gauge dimensions, the operating temperature range, a temperature compensation circuit, the transverse sensitivity (i.e. the strain perpendicular to the measurement axis), the strain magnitude of interest, and the fatigue characteristics of the gauge. Furthermore, ERS gauge rosettes, which consist of two or three gauges mounted at angles relative to each other, can also be used to measure the normal and shear strains on the surfaces of materials.

The use of ERS gauges requires attention to many details (Measurements Group 1983). A critical detail is bonding, because the adhesive must transfer the strain from the surface of the specimen to the gauge. Therefore, the adhesive must be compatible with both the specimen and the gauge materials.

The required curing temperature and curing time for the adhesive must also be considered. For example, some adhesives must cure at high temperatures, which may be unrealistic and unachievable for testing large wood specimens. During adhesive bonding, the gauge must be clamped to the specimen so that it achieves a rigid and permanent bond. The test environment, including the temperature and humidity, must also be considered when selecting an ERS gauge adhesive. Furthermore, the surface of the wood must be properly prepared by using an abrasive paper to expose a fresh wood surface before bonding.

The connection between the ERS gauge and the voltage measuring device is made by the lead wires, which must produce a precise, stable, electrical transmission. They must have low electrical resistance and, ideally, should be shielded from electrical noise by some sort of shielding and possibly by a braided wire to reduce electromagnetic flux. Flourescent lights, coiled extension cords, and radio noise all contribute to electromagnetic noise, which can affect ERS gauge readings.

The solder that is used to attach the wire to the ERS gauge must also have the proper operating characteristics

including melting temperature and fatigue. Proper soldering of the ERS gauge is important in producing a reliable and accurate measurement, and can only be acquired with practice. Because wood is a thermo-insulating material, ERS gauges tend to heat up due to the application of electricity to the circuit. On metal materials that conduct heat away from the gauge installation, the self-heating of the gauge is a minimal problem. On wood, however, because the heat is not rapidly conducted away from the gauge installation, the self-heating can appear as an apparent strain in the material. To minimize this effect for wood materials, an "active" and a "dummy" specimen are used. Two ERS gauges are bonded to the active specimen, which is loaded or stressed according to the user's needs. A matched dummy specimen of the same wood is located in the same test environment, and is also instrumented with two ERS gauges, but is not subjected to loads. These gauges are then arranged in the wheatstone bridge circuit so that the thermo-strains produced by self-heating are the same on both the active and the dummy ERS gauges and are automatically cancelled out by the electrical circuit.

Other operating characteristics are described in textbooks and literature provided by ERS gauge manufacturers (Measurements Group 1983).

Tell-Tale Gauges

Another type of gauge that may be useful for monitoring the long-term performance of stmctures is the tell-tale gauge. This gauge consists of two glass slides with etched micrometer grids. One end of one slide is mounted to the left side of a crack and the opposite end of the other slide is mounted to the right side of a crack. The two gauges are aligned so that the grid lines coincide as a zero position reading. If the crack in the building material opens or closes, or if the left or right side of the crack moves vertically relative to the other, the motion of the two glass slides will be apparent and can be manually read from the gauge. This type of gauge is relatively inexpensive and can be mounted in critical zones in buildings to discover if a crack is stable or if it is moving or growing. Applications include long-term monitoring of buildings, investigations of the stability of historic buildings, and other similar monitoring systems. These gauges have been used for years to monitor the performance of masonry materials and are relatively simple to use, are inexpensive, and have relatively high accuracy.

Conclusion

Accurate strain measurements require attention to many details. The characteristics of some traditional strain measuring devices, including extensometers, CET's, ERS gauges, and tell-tale gauges should be taken into consideration when deciding which type should be used in any particular application.

Literature Cited

Lang, E.M. 1993. Modeling the behavior of wood-based composite sheathing under hygrothermal load. Blacksburg. VA: Virginia Polytechnic Institute and State University. 177 p. Ph.D. dissertation.

Loferski, J.R.; Davalos, J.F.; **Yadama, V. 1989.** A laboratory built clip-on strain gauge transducer for testing wood. Forest Products Journal. 39(9): 45-48.

Measurements Group. 1983. Student manual for strain gauge technology. Bulletin 309B. Raleigh, NC: Education Division. 45 p.

Yadama, V.; Davalos, J.F.; **Loferski,** J.R.; **Holzer,** S.M. 1991. Selecting a gauge length to measure parallel-to-grain strain in southern pine. Forest Products Journal. 41(10): 65-68.

Image Correlation for Measuring Strain in Wood and Wood-based Composites

Audrey G. Zink, Robert W. Davidson, and Robert B. Hanna

Abstract

The suitability of a computer vision technique in experimental mechanics, known as the digital image correlation technique (DICT), for full-size test specimens of wood and wood-based composites was evaluated in this study. The technique utilizes digitized video images of undeformed and deformed test specimens and an image correlation computer routine to measure the displacements and strains of any or all points on the surface of the test specimens.

Evaluation was performed using axial compression and bending tests of small, clear specimens of wood and flexure tests of plywood and oriented strandboard specimens. A comparison of strain measurements obtained using an independent measurement technique and those obtained with the DICT showed close agreement.

Introduction

Full-field experimental measurements of the distribution of strain in wood have traditionally been tedious and difficult due, in part, to equipment limitations. Previously, brittle coatings, photoelasticity, Moire methods, and laser speckle interferometry have been investigated. Each of these methods requires surface treatments and/or modifications that change the mechanical properties on a local level or require complex, intensive, and expensive preparation and equipment. Because of the complexity and expense of these methods, examinations of only a few specimens are economically possible. Dial gauges, electrical strain gauges, and linear variable differential transducers have been the conventional devices for measuring point-wise strain in a wood specimen or structure. These devices measure strain over a very limited gauge length and, as a result, cannot be used for full-field measurements.

Audrey G. Zink is an assistant professor, Department of Wood Science and Forest Products, Virginia Polytechnic Institute and State University, Blacksburg, VA 2406 l-0323; Robert W. Davidson is a professor emeritus, Department of Wood Products Engineering, State University of New York, Syracuse, NY 13210; and Robert B. Hanna is a professor and Director, Center for Ultrastructure Studies, State University of New York, Syracuse, NY 13210.

The digital image correlation technique (DICT) is a full-field measurement method in experimental mechanics that has been developed recently as an application of computer vision. It relies on a mathematical correlation of digital images of the surfaces of test specimens acquired during mechanical testing. It has been employed to obtain quantities of interest in such diverse fields as rigid body mechanics (Sutton and others 1983), dynamics (Peters and Ranson 1982), experimental mechanics (Chu and others 1985), fluid mechanics (He and others 1984), and biomechanics (Ranson and others 1986). The technique has been applied to a vast range of loading, environmental, and testing conditions and materials. Because of its advantages and wide spread application, the technique is rapidly becoming well established in experimental mechanics. The applicability of the DICT for measuring strain in full-sized specimens of wood and wood-based composites is discussed in this paper.

Background

Peters and others (1989) and Sutton and others (1983) have shown that the use of white light illumination of a random, black and white pattern made it possible to obtain strain measurements with optical techniques in conjunction with a digital computer. In this research, they developed extensive mathematical and experimental techniques for cross-correlating a reference image with a stored image for application in experimental mechanics. This cross-correlation technique is similar to area correlation in pattern recognition methodology. The cross-correlation of two functions is used to indicate the relative amount of agreement between the two functions for various degrees of shifting. In the case of experimental mechanics, the displacement imposed on the test object during mechanical loading is measured as the degree of shifting of the light intensity patterns as found by the cross-correlation criterion.

Recently, Choi (1990) and Choi and others (1991) have examined the experimental application of DICT by utilizing video microscopy and obtaining surface randomization using carbon photocopy toner particles for the measurement of displacement and strain in small specimens of wood and paper. This application showed that the DICT could be a fast, simple, and accurate method when applied to very small specimens of wood (1 by 1 by 4 mm in size) and to paper. Full-field deformation of wood test specimens using laser speckle interferometry and digital image processing was applied by Agrawal (1989) to study the suitability of the system for monitoring the creep response of wood. Excellent comparisons were shown between strain measurements obtained with the image correlation technique on wood and several independent measurement devices such as strain gauges (Agrawal 1989) and a Mann comparator (Choi 1990).

Experimental Procedures

The Digital Image Correlation Technique

Equipment-The equipment used to acquire and digitize the video images was a black and white Panasonic' WV–CD50 CCD camera and a Coreco® Oculus-200 real-time, gray-level, image digitizer board in an IBM' personal computer (PC). The matrix resolution for this particular board was 480 by 5 12 picture elements, called pixels. The lens used with the video camera was a Nikon® 55-mm macro lens. A standard C-mount adapter was used to attach the macro lens to the video camera. A high resolution Panasonic' video monitor, model BT-S 1300N, was used to display the digital image. The illumination source was a 22-W, circular, fluorescent tube suspended and centered around the camera. The illumination of the surface was carefully controlled by surrounding the testing machine table and the camera with two layers of heavy black cloth and cardboard, and extinguishing all room lights.

The PC and image digitizer board system was used to digitize the video images, redisplay them on the video monitor for focusing and brightness control, and then transfer them to a mainframe computer for analysis with the image correlation computer routine as described in a following section.

The CCD video camera recorded the surface light intensity pattern as varying levels of gray. To digitize the video signal that represented the light pattern, the video image was divided into an array of equal-area, rectangular pixels. The gray level of each pixel was assigned an integer value from 0 to 255 that was proportional to the light intensity received from the surface of the test object. The lowest intensity (black) was assigned 0, and the highest (white) was assigned 255, with values in between representing different shades of gray. The integers representing the light intensity pattern of the test object were assigned pixel locations based on an X-Y coordinate system that corresponded to the actual location on the test object.

Correlation Analysis-The digitization process represented the continuous, light intensity patterns of the recorded images in a discrete numeric form. Because a pixel in undeformed coordinates may relocate to positions between pixels in deformed coordinates, an interpolation of gray levels between pixels was needed to represent the original continuous pattern. A bilinear interpolation scheme was used in this study.

The digitized intensity pattern after deformation was related to the digitized, interpolated, intensity pattern recorded before deformation. A mathematical correlation of the two images to determine image differences allowed for determining the object displacement. The image correlation program compared subsets of digitized, light intensity values of subregions around selected pixels in the undeformed images with all subregions of the same size in the deformed image.

In this study, the correlation analysis was carried out on an IBM@ 3090 mainframe computer and a Cray® Y-MP supercomputer at the Pittsburgh Supercomputing Center. The analysis selected subregions to find the values of six unknown parameters that minimized the correlation function, C; C is a nonlinear function dependent on the subregion size and the unknown parameters and is unique for each selected pixel location. The correlation function to be minimized was the sum of the squares of the differences of the light intensity values of the subregions in the pairs of images and is a "least squares" correlation to measure how well the subsets match. It is written:

$$C(u, v, \delta u/\delta x, \delta u/\delta y, \delta v/\delta x, \delta v/\delta y) = \sum_{M} [A(x,y) - B(x',y')]^2 \quad (1)$$

where

u and v = the displacements for the subset centers in the x and y direction, respectively,

A (x, y) = the gray-level value at coordinate (x, y) in the deformed image,
B (x', y') = the gray-level value at point (x', y') in the undeformed image, and
M = the subregion of interest chosen from the digital images.

The subregion, M, used for the correlation comparison was 20 by 20 pixels in size and centered around the selected measurement points. A subregion of this size was chosen to minimize the effects of local wood-structure deviations, to minimize image distortion, to reduce correlation time, and to obtain a pattern that was statistically different from its neighbors.

The coordinates (x,y) and (x',y') are related by the deformation that occurred between acquisition of the two images as imposed by the mechanical loading. If the motion of the object relative to the camera is parallel to the image plane and the deformations are small, the images are related by

$$x' = x + u + (\delta u/\delta x)(\Delta x) + (\delta u/\delta y)(\Delta y), \text{ and} \quad (2)$$

$$y' = y + v + (\delta v/\delta x)(\Delta x) + (\delta v/\delta y)(\Delta y) \quad (3)$$

where

u and v = the displacements for the subset centers in the x and y directions respectively, and
Δx and Ay = the distances from the subset center to the point (x,y).

The correlation of the images was obtained by determining the values for the six unknown parameters: u, v, $\delta u/\delta x$, $\delta u/\delta y$, $\delta v/\delta x$, and $\delta v/\delta y$, which minimize the correlation coefficient, C. Minimization of functions, or optimization as this procedure is often called, is a very large area of numerical research. Various schemes exist for achieving this minimization in the literature on image correlation. In general, a coarse-fine search technique for determining the minimum or best fit value has been used. This procedure requires a very large number of calculations and is very computationally intense.

A new method for obtaining the best fit was evaluated in this study: the quasi-Newton method. This method was used to provide the successive approximations of the initial guesses of the six unknown deformation parameters. A two-parameter model was iterated until all values were within the tolerance limits. The values of the six unknown parameters that minimized the correlation function were returned as the best approximations to the six deformation parameters. This method provided convergence with fewer calculations and, therefore, greatly decreased the computational time.

In this study, a typical correlation analysis was conducted on a measurement matrix of 23 points parallel to the load axis and 11 points perpendicular to the load, for a total measurement grid of 253 points. The results of the correlation analysis were the displacements parallel and perpendicular to the load of the virtual measurement grid of the 253 points. Once the displacement of the selected points was determined, the strain was calculated as the relative displacement of the points divided by the original distance between the points. With this technique, the normal and shear strains are measured, and from these strains, the modulus of elasticity and Poisson's ratio can be calculated.

Distortion from out-of-plane effects was minimized by working with low magnifications (<3X), a high-quality lens with a large depth of field, and specimen-to-lens working distances of >400 mm. Sutton and others (1990) have determined that magnification of <5X and a distance from the camera lens plane to the object of >400 mm is sufficient to reduce to an acceptable range any distortion from out-of-plane movement of the specimen. They determined that, at these levels, any noise that appears in the displacement fields is from sources other than out-of-plane effects.

The displacements due to external loading were measured with an image correlation measurement matrix of 20 points perpendicular to the load (x-direction) and 15 points parallel to the load axis (y-direction). Each of the points was placed at 20-pixel intervals on the computer image for corresponding gauge lengths of 3.85 mm in the x-direction and 1.33 mm in the y-direction on the test specimen. The computer-image measurement grid of 300 points was located in the central portion of the image to minimize edge effects and curvature of the field.

The normal strains (ϵ_{xx} and ϵ_{xy}) between each measurement point were calculated as the change in distance between the points in the x-direction or y-direction divided by the original distance between the points ($\Delta L_x/L_x$ and $\Delta L_y/L_y$). This change in distance between the points was determined using the displacements of each point as measured with the image technique. The shear strain (ϵ_{xy}) was calculated as the change in angle between adjacent sides of an elementary block, defined by four measurement points, as this block was distorted under shearing stresses. The change

in angle was determined using the displacements of each of the four points as measured with the image technique.

A finite difference method that utilized a forward difference scheme was employed for the strain field calculations. The strain values in the following contour plots were calculated using the image acquired at a slight preload as the reference image. As a result, the strain values in each figure represent the strain that accumulated from the onset of that initial load up to the load at which the images were acquired. The average standard deviation in strain was 0.00027.

Calibration and Evaluation-Extensive evaluation and calibration procedures were carried out on the experimental equipment and image correlation computer program. Calibration tests were conducted on an aluminum alloy block and a small, clear specimen of wood. Aluminum was used for calibration because it is considered a typical, isotropic, homogeneous, elastic material whose elastic constants are accurately known and can be used for comparison. Testing to determine system noise levels involved acquisition of images at several time intervals and determination of the differences of the digital gray values between these images. A carbon speckle pattern was applied to the surface of an aluminum alloy block, the block was placed on the table of the testing machine, and images of the entire surface were acquired over time. No load was applied to the specimen during this experiment, none of the equipment was moved, and the light was left on throughout the experiment. Four 20 by 20 subsets of digital gray values were chosen at random locations on the surface of the aluminum block for each time interval and compared to the reference image acquired at time zero. There were no apparent strains in the 60 minutes allowed for this testing.

Accuracy and precision estimates were determined by comparing strains obtained with the vision system and the strains as measured with a compressometer that had been carefully calibrated to a secondary standard with known accuracy. The accuracy of the vision system was calculated as the maximum deviation of the readings from this known standard. The precision was calculated as the maximum deviation of several readings from the mean of those readings.

The electronic device used for the calibration was a Daytronics® DS 190V linear variable differential transducer (LVDT). The LVDT was carefully calibrated just prior to testing using a T63R1Starrett® micrometer head. The Starrett® micrometer had been calibrated within a year of use according to master standard National Institute of Standards and Testing Test 7311241460 and in accordance with MIL-STD-45662A and MIL-I-45208A. Both the precision and accuracy of the micrometer were found to be ± 0.127 mm. The full scale of the micrometer was 5.08 cm. The precision and accuracy of both the micrometer and the LVDT in terms of their percentage of full-scale reading were found to be 0.0025 percent. Axial strain was measured relative to the same gauge length for both techniques. The test was replicated 10 times. It was determined that both the precision and accuracy of the computer vision system was ho.0025 percent of a full-scale reading of 5.08 cm. Figure 1 illustrates the plot of a typical calibration curve for the two independent measuring systems.

Specimen Preparation

Fabrication-Small, clear, test specimens of sugar pine (*Pinus lambertiana* Dougl.) and red oak (*Quercus* spp.) were prepared for compression and bending testing in accordance with American Society for Testing and Materials (ASTM) D143-83 Standard Methods of Testing Small Clear Specimens of Timber (1983). Thirty sugar pine and 30 red oak compression specimens were prepared. The test specimens were 2.54 by 2.54 cm in cross section and 10.16 cm along the grain. Sixteen bending specimens were prepared from the same boards of sugar pine and red oak. The bending specimens were 2.54 by 2.54 cm in cross section and 40.64 cm along the grain. The average initial moisture content of the specimens was 8.5 percent.

Flexure specimens of live-ply, 48124 American Plywood Association (APA) Rated Sheathing plywood and APA Rated Sturd-I Floor@ oriented strandboard (OSB) specimens were prepared in accordance with ASTM D3043-87 (Reapproved 1993) Standard Method of Testing Structural Panels in Flexure (1987). Four flexure specimens were prepared from the plywood and the OSB. The plywood specimens were 5.08 cm across and had a test span of 144 cm. The OSB specimens were 5.08 cm across with a test span of 76.2 cm.

Carbon Speckle Application-Because the image correlation technique used to determine the strain distributions relies on a comparison of discrete, light intensity patterns obtained before and during deformation to reveal the shift of the images, a unique, random intensity pattern is required on the surface being observed. Wood specimens, in general, do not provide the required, unique, sharp contrast patterns. In this study, the contrast was enhanced with toner particles used in standard photocopy

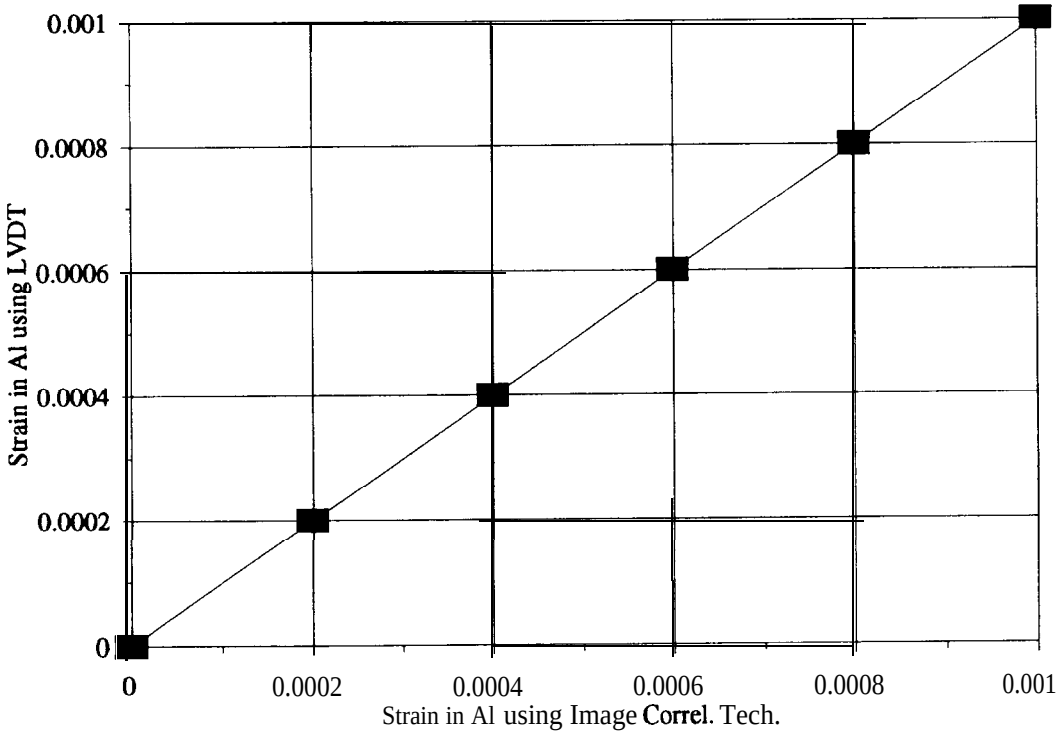

Figure l-Calibration curve for two independent systems measuring strain in an aluminum block.

machines. The particles are distinctly black in hue and contain carbon black and chrome III pigments.

The unique contrast pattern was created on the surface of the wood and composite specimens with a light speckle of carbon particles. The particles were sifted through a screen held above the surface of the specimen and scattered across the surface by room air currents. Heat was applied to the carbon particles using a heat lamp. The particles melted and flowed into the wood structure after 10 minutes in an air temperature of approximately 70 "C. The specimens were then allowed to cool. During the cooling process, the particles solidified and became tightly anchored to the wood structure. The advantages of this particular speckle pattern are that it does not mask the underlying wood structure and it does not modify the material properties of the test specimen in any manner.

Moisture Conditioning-The test specimens were conditioned to approximate the equilibrium moisture content in the testing laboratory using an Amino-Aire® humidity-temperature control chamber. The specimens were weighed periodically until no weight change was noticeable and kept in the chamber at constant conditions until just prior to testing. The average moisture content of the specimens just prior to testing was 12 percent as determined by ASTM Standard D4442-92 Standard Test Methods for Direct Moisture Content Measurement of Wood and Wood-base Materials (1992).

Mechanical Testing

Compression and Static Bending Tests-A Baldwin-Emery@ SR-4 universal testing machine was used for the testing of the compression and bending specimens, following ASTM D143-83 methods (1983). The compression load was applied parallel to the grain. The bending tests were conducted with a single, center-point load. The load data were acquired during the tests using an IBM® Model 5 150 PC and a Hewlett Packard@ 6621A system direct-current power supply. The sampling rate was 2 Hz. The displacement data were recorded using the DICT described earlier in this report.

Flexure of Wood-Based Composite Panels-An Instron® testing machine was used for the testing of the composite specimens, following ASTM D3043-87 (1987). The specimens were simply supported and a center-point load

was applied to the wide face of the specimens. The load data were acquired using the data acquisition system listed above. The displacement data were recorded using the image correlation technique over the center 10 cm beneath the load head.

Results and Discussion

Compression and Static Bending Tests of Solid Wood

Compression-Figure 2 illustrates a typical strain plot obtained from compression parallel to the grain. Figure 2a is the plot of the strains parallel to the load, and figure 2b is the strain plot perpendicular to the grain. These strain plots were acquired just prior to ultimate failure of the specimen. An examination of figure 2a indicates that the distribution of the strain parallel to the load is not as homogeneous as might be expected. The unique microscopic features of the wood elements are responsible for the nonhomogeneous nature of the strain fields. The location of the highest strain on the strain plots parallel to the load exactly corresponds to the location of visible failure lines on the test specimen. An examination of figure 2b indicates that there are strains perpendicular to the load, which is experimental confirmation of the Poisson effect in wood. This strain distribution is also nonhomogeneous due to the underlying, microscopic, anatomical, arrangements. The location of the highest strain also corresponds to the location of failure on the test specimen.

Bending-Figure 3 is an example of the strain distributions obtained from bending a small, clear specimen of wood. Figure 3a is a plot of the strains perpendicular to the load (along the axis of the beam), and figure 3b is a plot of the strains parallel to the load. The strain plots were acquired just prior to failure of the beam. The highest strains in these plots are just beneath the load point, the distribution of strain across the face of the beam is symmetrical, and the neutral axis is approximately middepth. None of these results were unexpected; however, it had never before been possible to measure the distributions in as much detail and with as much accuracy prior to this study using the image correlation technique. The failures of the beam were in exact correlation with the locations of the highest strains on the strain plots.

Flexure of Wood-Based Composite Panels

Plywood-Figure 4 is an example of typical strain plots obtained from flexure of plywood specimens. Figure 4a is a plot of the strains perpendicular to the load (along the axis of the beam), and figure 4b is a plot of the shear strains on the surface of the beam. The load level is approximately 50 percent of the ultimate load. Examination of these plots indicates an accumulation of high strain at a load of only half the ultimate load. These plots further indicate what would be expected from theoretical mechanics: compression strains, tension strains, a neutral axis where expected, a linear distribution of axial strains, and strain concentrations near the loading point. It has not been possible until now to verify these expectations. Traditionally, plywood has been considered as a solid, homogeneous structure. However it was discovered in this study that, by overlaying these strain plots on the actual failed specimen, each ply of the composite board was acting as an individual beam and there was shear at each glueline.

Oriented Strandboard-Figure 5 is an example of typical strain plots from the flexure of OSB. Figure 5a is the plot of strains perpendicular to the load (along the axis of the beam), and figure 5b is a plot of the shear strains on the surface of the OSB. These strain plots were acquired at approximately 75 percent of the ultimate load. An examination of the strains along the beam (fig. 5a) indicates that the distribution is not symmetric, the neutral axis is not a straight line, most of the strain occurs near the lower edge of the beam, and regions of compression extend well below middepth. These results might be explained in part by the localized compaction of the strands in the region of the load point and by each strand acting as an individual beam. An examination of the shear strains (fig. 5b) also indicates that OSB behavior does not follow expected patterns. The shear strains are maximum near the surface, and the distribution has left/right symmetry with a central neutral region from the top to the bottom of the specimen. When overlaid on the actual test specimen, the strain distributions indicated some correlation with the location of the individual strands of the composite. The test specimen failed due to adhesion failure, allowing the separation of individual strands, rather than to the cohesion failure of the wood. Further tests are being conducted on the composite boards.

Conclusions

The image correlation technique was shown to be an accurate, simple, and versatile method of measuring strain distributions in wood and wood-based composites. The technique is noncontact and is not limited by the size or

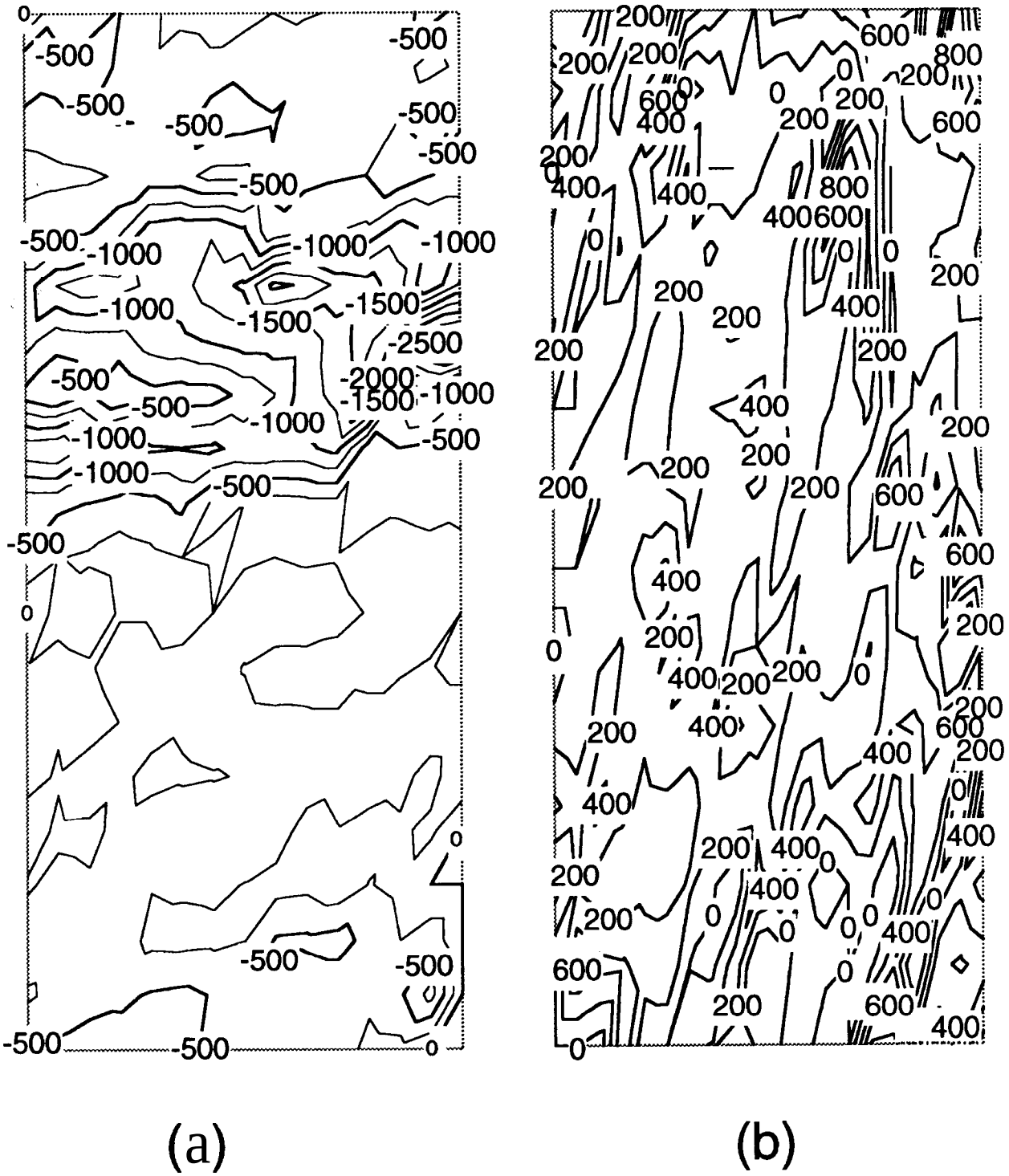

Figure 2-Strain contour plots for compression test specimen at a load level of 18.6 kN; (a) strain perpendicular to the grain; (b) strain parallel to the grain (strains are shown x 10^{-6}).

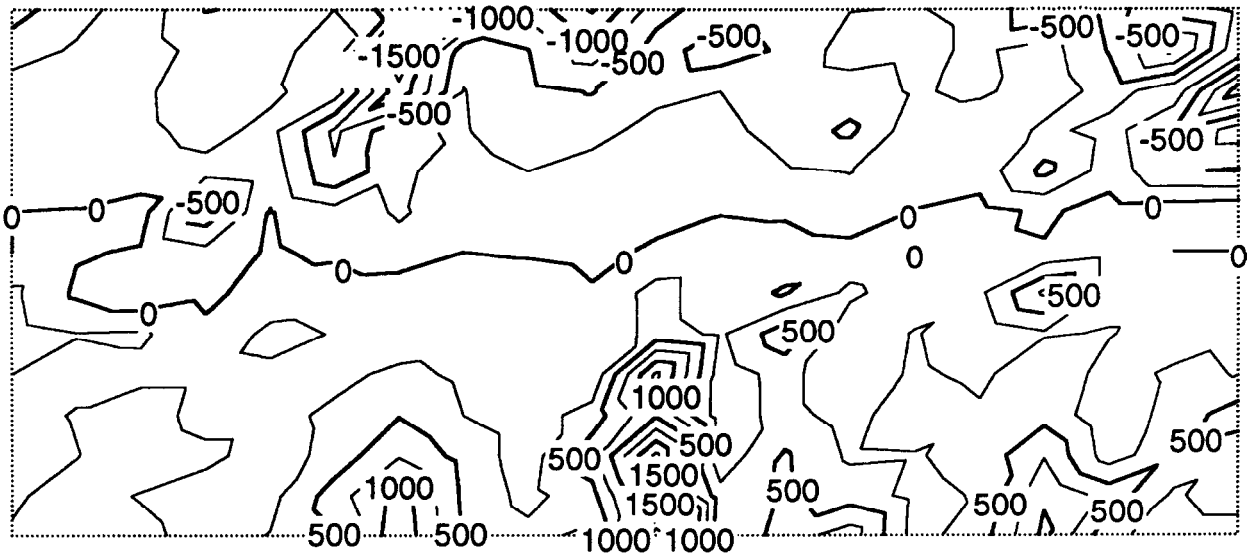

(a)

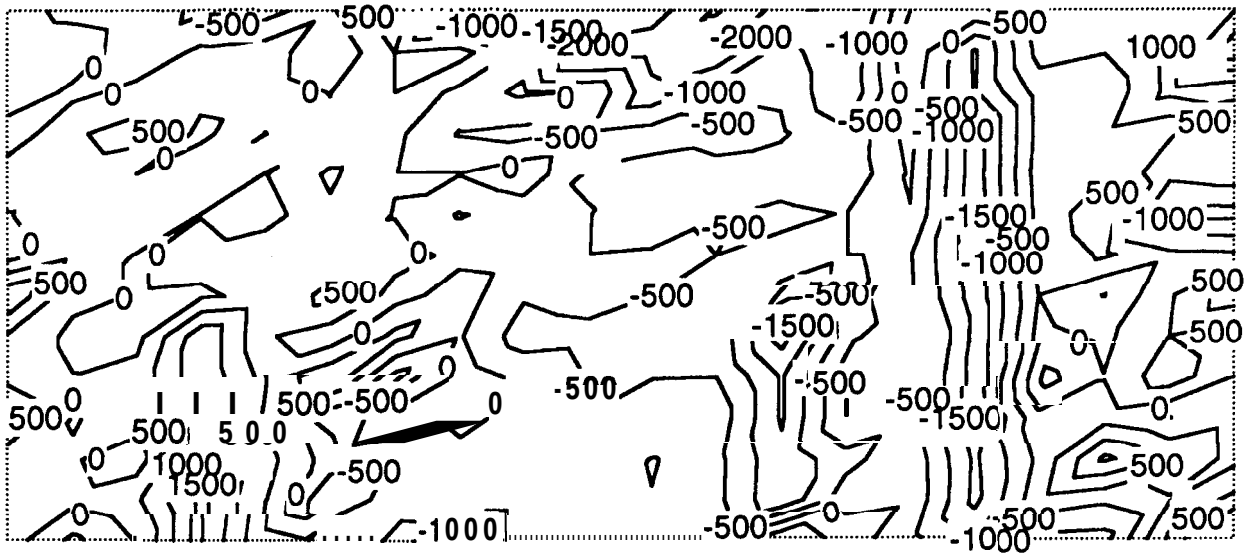

(b)

Figure 3—Strain contour plots for bending test specimen at a load level of 1.3 15 kN; (a) strain perpendicular to the grain; (b) strain parallel to the grain (strains are shown at $x10^{-6}$).

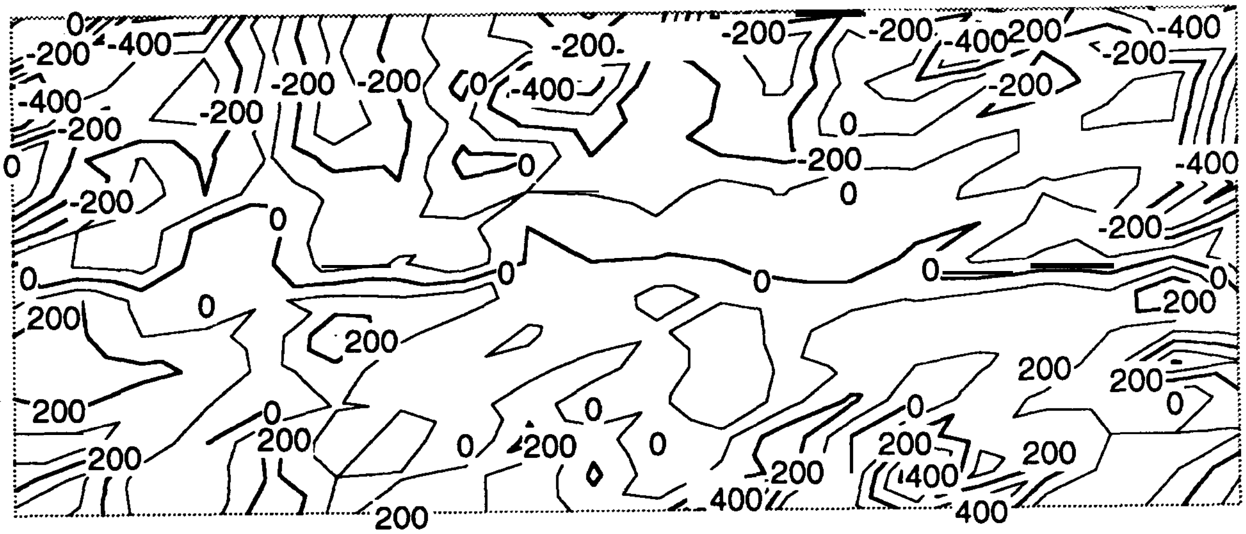

(a)

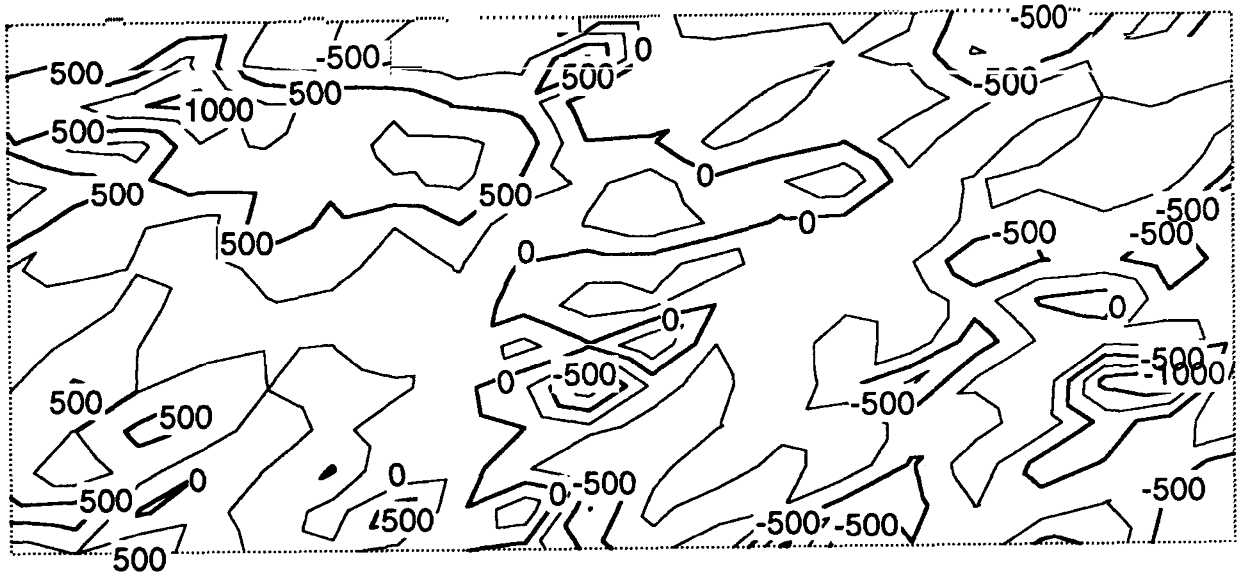

(b)

Figure &Strain contour plots for plywood flexure specimen at a load level of 0.243 kN; (a) strain perpendicular to the grain; (b) shear strain (strains are shown $x10^{-6}$).

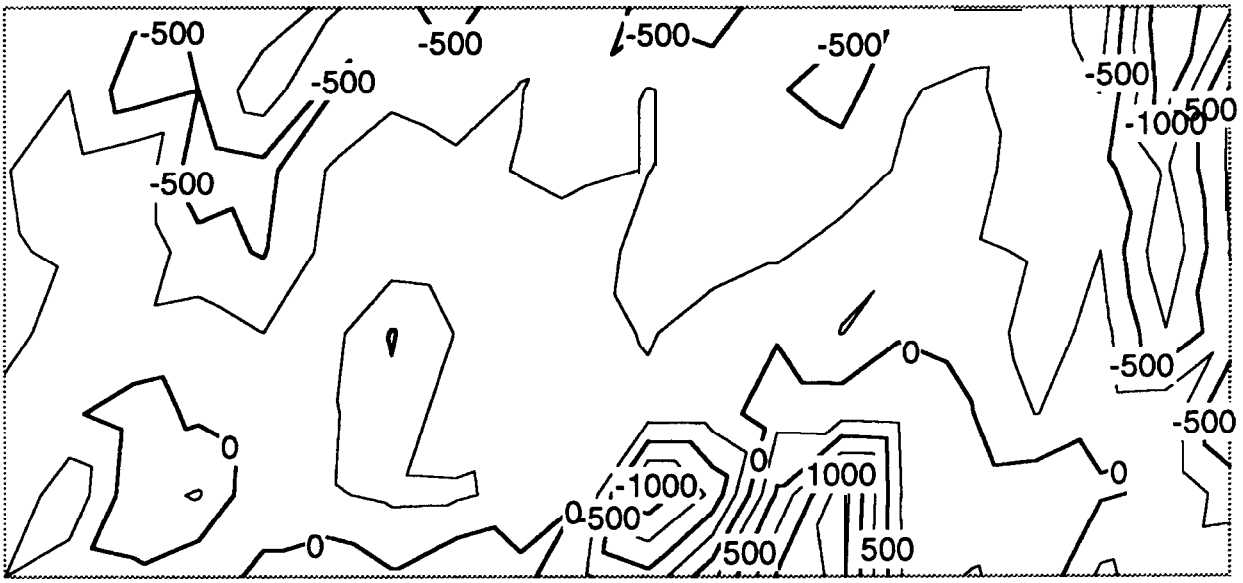

(a)

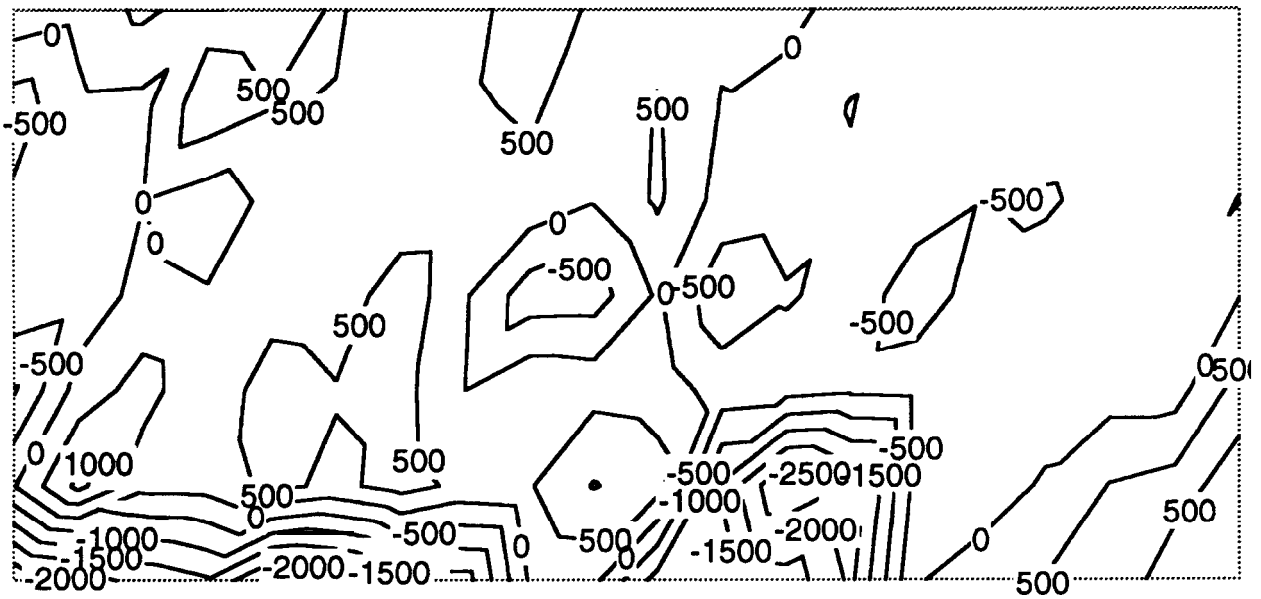

(b)

Figure 5—Strain contour plots for oriented strandboard specimen at a load level of 0.285 kN; (a) strain perpendicular to the grain; (b) shear strain (strains are shown $\times 10^{-6}$).

nature of the specimen. The distributions of strain in the compression tests was nonhomogeneous due to the unique anatomical structure of wood. The strain distributions from bending tests on small, clear specimens of wood indicated close agreement with conventional beam theory and exact correlation with the failure pattern of the specimen. However, neither composite board followed conventional beam theory entirely. Of the two composites investigated in this study, the plywood exhibited behavior closer to conventional theory. The OSB exhibited strain patterns very closely related to composite structure arrangement.

Acknowledgments

The authors are grateful to Mr. Arnold C. Day and Mr. John McKeon, State University of New York, Syracuse, New York, for their technical assistance, Dr. Wayne E. Fordyce, Syracuse University, Syracuse, New York, for his assistance with the correlation analysis, and the USDA McIntire-Stennis Forest Research Program for financial assistance.

Literature Cited

Agrawal, C.P. 1989. Full-field deformation measurements in wood using digital image processing. Blacksburg: Virginia Polytechnic Institute and State University. 103 p. M.S. thesis.

American **Society for Testing and Materials. 1983.** Standard methods of testing small clear specimens of timber. ASTM Standard D143-83. Philadelphia, PA. ASTM. 57 p.

American Society for Testing and Materials. 1987. Standard method of testing structural panels in flexure. ASTM Standard D3043-87 (Reapproved 1993). Philadelphia, PA. ASTM. 11 p.

American Society for Testing and Materials. 1992. Standard test methods for direct moisture content measurement of wood and wood-base materials. ASTM Standard D4442-92. Philadelphia, PA. ASTM. 5 p.

Choi, **D.** 1990. Failure initiation and propagation in wood in relation to its structure. Syracuse: State University of New York. 149 p. Ph.D. dissertation.

Choi, D.; Thorpe, J.L.; Hanna, R.B. 1991. Image analysis to measure strain in wood and paper. Wood Science & Technology. 25: 251-262.

Chu, T.C.; Ranson, W.F.; Sutton, M.A.; Peters, W.H. 1985. Applications of digital image correlation techniques to experimental mechanics. Experimental Mechanics. 25(3): 232-244.

He, **Z.H.; Sutton,** M.A.; **Ranson,** W.F.; **Peters,** W.H. 1984. Two-dimensional fluid-velocity measurements by use of digital speckle correlation techniques. Experimental Mechanics. 24(2):117-121.

Peters, W.H.; Ranson, W.F. 1982. Digital imaging techniques in experimental stress analysis. Optical Engineering. 21(3): 427-431

Peters, W.H.; Sutton, M.H.; Ranson, W.F.; [and others]. 1989. Whole-field experimental displacement analysis of composite cylinders. Experimental Mechanics. 29(l): 58-62.

Ranson, W.F.; Walker, D.M.; Caulfield, J.B. 1986. Biomechanics. In: Computer vision in engineering mechanics: a discussion paper prepared for the NSF workshop on solid mechanics related to paper; [dates unknown]. Blue Mountain Lake, NY [Place of publication unknown]. [Publisher unknown]: [pages unknown].

Sutton, M.A.; **Chae,** T.L.; **Turner, J.L.; Bruck, H.A. 1990.** Development of a computer vision methodology for the analysis of surface deformation in magnified images. ASTM STP 1094 Micon 90. Philadelphia, PA. ASTM: 109-132.

Sutton, M.A.; Wolters, W.J.; Peters, W.H.; [and others]. 1983. Determination of displacements using an improved digital correlation method. Image and Vision Computing. l(3): 133-139.

Application of Imaging Technologies to Experimental Mechanics

Laurence Mott, Stephen M. Shaler, and Leslie H. Groom

Abstract

Digital image technologies are rapidly emerging as a powerful adjunct to traditional experimental mechanics techniques. The essential hardware components as well as considerations in their selection are described in this paper. A historical perspective of imaging applications to the testing of individual wood fibers is essential to understand these technologies. Additionally, examples of results obtainable from new imaging microscopes (the environmental scanning electron microscope and the confocal laser scanning microscope) show quantum leaps in the level of detail now possible. The combination of these image acquisition systems with image analysis techniques, such as digital image correlation, is proving to be a powerful tool for quantifying and understanding the microstructural character of wood composite materials.

Introduction

As is the case with any productive manufacturing sector, success and growth of the forest products industry relies heavily on research. Staying abreast of current technologies is crucial to developing new forest products, improving product quality, and increasing the efficiency of processing. Digital processing advancements in recent years have led to a myriad of new experimental techniques that take advantage of this newfound computing power. One of the fastest growing areas of experimental techniques is that of digital image acquisition and processing.

Digital image processing in its various forms is now commonly employed in the forest products industry. However, image forming and processing technology is developing at such a rapid rate that only people directly involved with it can hope to keep abreast of the latest innovations. Some of the most exciting forest products research couples digital image processing with improved microscopic capabilities. Some of the new image forming technologies such as environmental scanning electron microscopy and confocal laser scanning microscopy can provide precise and accurate quantitative information and data that were previously unattainable or obtainable only by some less reliable method. Such techniques allow the forest products industry to determine fundamental knowledge of material behavior in composite systems.

Laurence Mott is a graduate research assistant, Department of Forest Management, University of Maine, Orono, ME 04469; Steven M. Shaler is an associate professor. Department of Forest Management, University of Maine, Orono, ME 04469; Leslie H. Groom is a research technologist, USDA Forest Service, Southern Research Station, 2500 Shreveport Highway, Pineville, LA 7 1360.

Digital Imaging Techniques

There are three basic forms of imaging techniques applicable to experimental mechanics: analog signals, solid state/tube cameras, and noncamera systems such as scanning electron microscopes (SEM's). First, some of the early imaging techniques that relied on an analog signal will be appraised. Second, the establishment of simple digital imaging systems will be illustrated, with key considerations involved in hardware/software compatibility being identified. Finally, noncamera-based, digital, imaging systems and their usefulness in the field of experimental micromechanics will be discussed.

Traditional Techniques

Some of the earliest imaging techniques were used primarily to qualitatively observe failure processes. McMillin (1974) examined failure mechanism of individual wood fibers loaded in torsion. The sequence shown in figure 1 was recorded with Polaroid@ film and was useful in studying the torsional failure mechanism. Page and others (1977) used a 16-mm cinemagraphic camera to acquire images of individual fibers loaded in tension (fig. 2). The images could be matched with load-elongation traces to ascertain the fiber response to loading. These early attempts at image acquisition were an important first step in studying fracture behavior because they allowed the classification of fracture mechanisms and provided an

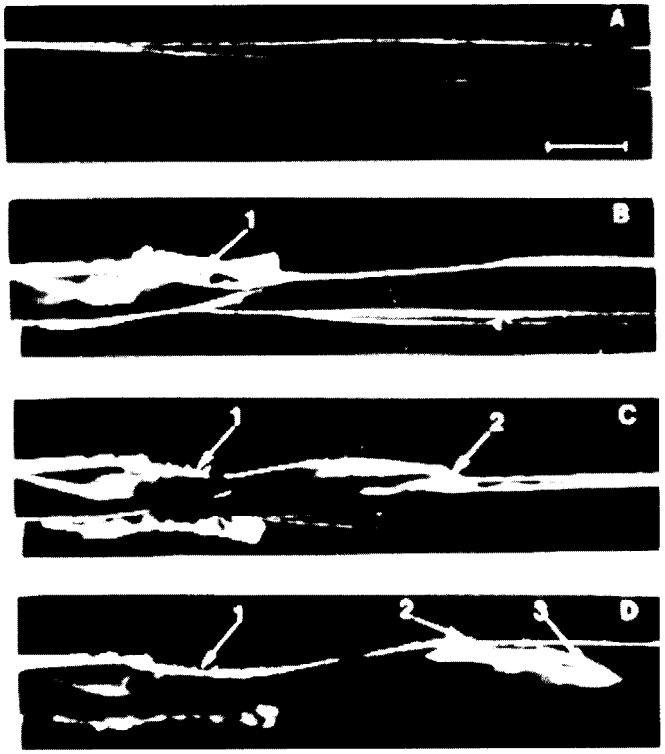

Figure l-Failure sequence (from A to D) of a latewood tracheid subjected to torsional loading recorded with Polaroid' film. The scale bar in A equals to 50 pm and is also applicable to B, C, and D *(photo courtesy of C. McMillin).*

understanding of basic, fundamental, material properties. Although cinemagraphic and Polaroid@ films are useful for observing behavior, they are of limited use due to handling and processing problems, the analog nature of the image, and the relative high cost of each image.

Digital Imaging Systems

Digital image processing offers several advantages when compared to comparable analog systems. The digital format allows for quantitative measurements between images as well as further processing after images have been acquired to improve their quality through brightness and contrast enhancement. Digital images are inexpensive, easily obtainable with commercially available equipment, and limited only by the amount of available disk storage space.

One of the first considerations for a basic digital imaging system is the camera. There are two basic types of cameras: tube (sometimes referred to as Vidicon®) cameras and solid-state [more commonly referred to as charge-coupled device (CCD)] cameras. Vidicon' tube cameras typically possess high resolution attributes, such as 1,600+ television lines per 2,000 pixels as well as high sensitivity (ISIT and SIT tubes) with up to 1,000 times more spectral sensitivity than conventional CCD cameras. However, the Vidicon®

(A)

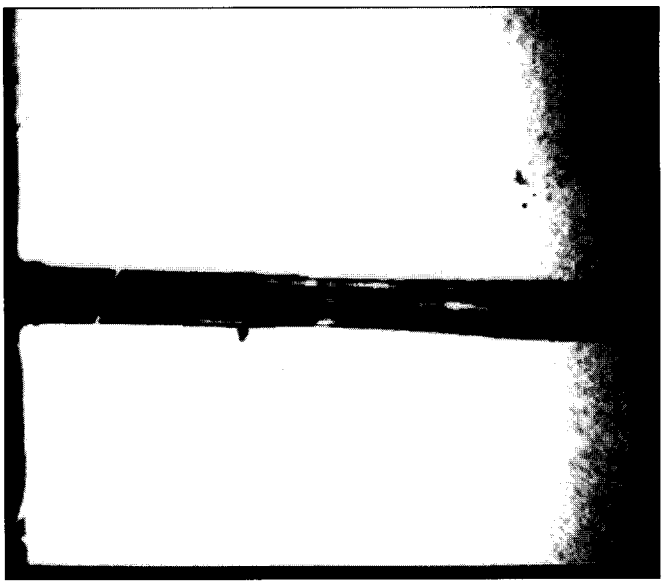

(B)

Figure 2—Cinemagraphic images of a single tracheid fiber; (a) subjected to low load levels; and (b) at prefailure. Load-elongation traces are shown as a ghost image in each photo (*photos courtesy of D.H. Page).*

tube cameras also have several major disadvantages: They require frequent adjustments and maintenance, they are more expensive while being less rugged and reliable than CCD cameras, and they have a continuous analog system that requires a compatible framegrabber, which can be costly.

The relatively low cost and commercial availability of CCD cameras make them the most common camera type in a digital imaging system (fig. 3). There are several factors to consider when choosing a CCD camera. The cost of the camera is proportional to its resolution, so the highest resolution camera within the available budget should be chosen. There are several sizes of CCD chip formats ranging from 6 mm to 25 mm. Generally, smaller sized chips have better resolutions than larger chips given the same number of pixels. The lens size must be chosen so as to complement the chip size of the CCD camera. The operating light level and signal-to-noise ratio should also be considered. Although most imaging systems utilize a black-and-white camera, color cameras are also available. Color cameras cost about three times as much as comparable black-and-white cameras. In addition, the accompanying framegrabber for the color CCD camera is several times the cost of a conventional black-and-white framegrabber.

Conventional CCD systems are used primarily to measure the areas and light intensities of digital images of interest. An example is the work by Mercado (1992) in which he modified a standard digital imaging system to measure half-fringe photoelasticity. He was able to measure the interfacial shear stress between a polymer matrix and an embedded wood fiber by measuring the photoelastic effect (or light intensity) of the polymer sheet (fig. 4).

Micromechanical studies are generally interested in specimen deformations. The translation and deformation of a solid body can be measured by user-written algorithms referred to as digital image correlation (DIC) (Chu and others 1985). The accuracy of in-plane deformations can be corrupted by translations perpendicular to the camera. Binocular systems can be designed that use two cameras placed at a predetermined distance from each other and, when used in conjunction with DIC, allow a three-dimensional (3D) analysis of both rigid and deformable bodies (Luo and others 1993).

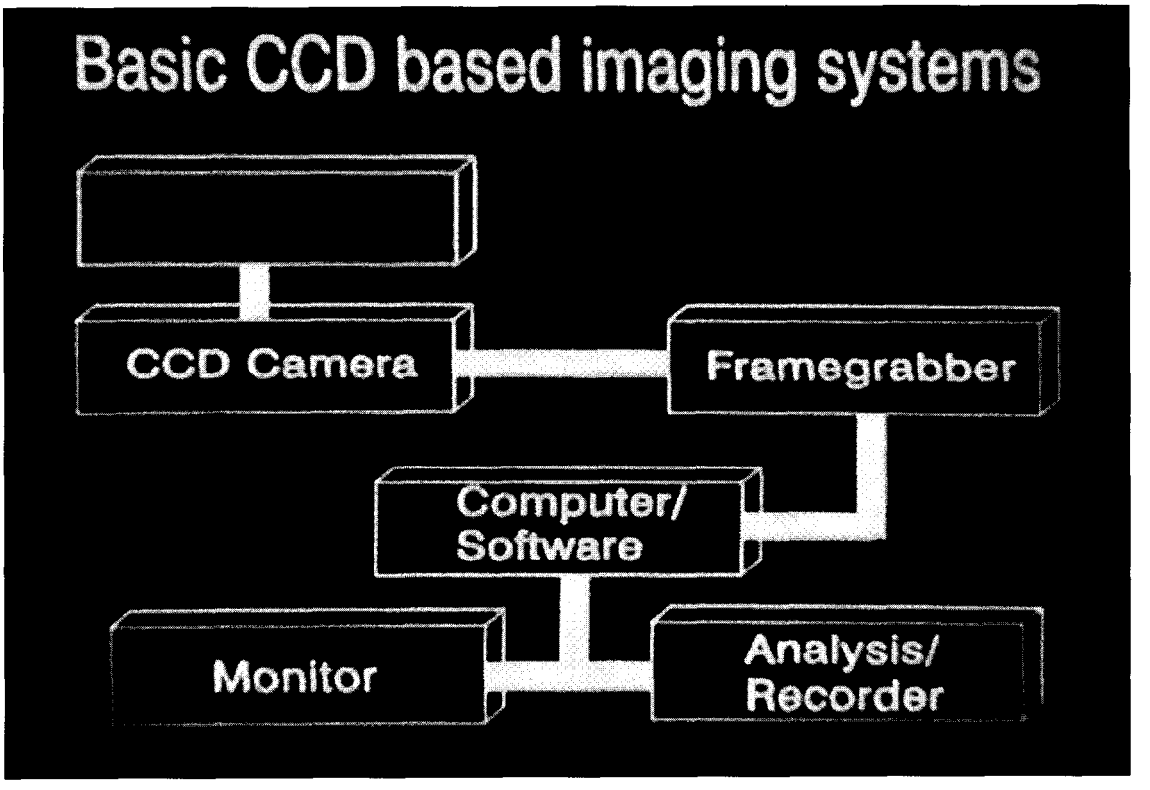

Figure 3—Schematic design for a basic digital imaging system.

Figure 4-Digital image of an individual wood fiber embedded in a polyurethane sheet as seen under a circular polariscope. Fringe patterns are indicative of stresses in the polymer sheet.

An advanced digital imaging system is necessary when obtaining confocal laser scanning microscope **(CLSM)** images. A **CLSM** system uses laser light, a conventional light microscope, and a controlled XYZ stage to produce 3D images. The 3D image is actually a computer-built composite of individual images from only in-focus planes. Laser light can penetrate a translucent material, thus focusing is possible only if the object is small enough and is transparent enough. The 3D images can generally be rotated to any angle in the X, Y, or Z direction. Figure 5 shows a loblolly pine, earlywood fiber that was scanned longitudinally (XY section), with the image then rotated 90 degrees such that the fiber cross section (YZ section) is exposed. Morphometric measurements can then be made to determine the cross-sectional area as well as the cell wall thickness at any point along the length of the wood fiber. This technique was recently used by Hamad [in press] to visualize crack formation within fiber walls due to fatigue loadings.

Noncamera-based Imaging Systems

The most classic example of a noncamera-based imaging system is the SEM. Wood-based specimens placed within the chamber of a standard SEM need to be coated with a conductive material (e.g., gold) and are subject to very high vacuums that lead to unrealistic test conditions. Standard SEM's are thus limited to static or postfailure specimens. The environmental SEM (ESEM) has several advantages over a standard SEM: the specimen chamber can contain a gaseous environment and may be kept at a pressure and temperature that permit water to exist in a vapor and liquid state. In addition, materials can be observed in a natural, nondehydrated state, no conductive coating is necessary, and dynamic testing is feasible.

The combination of a high degree of surface contrast, a high magnification, and a realistic environment make the ESEM a very useful tool for examining failure

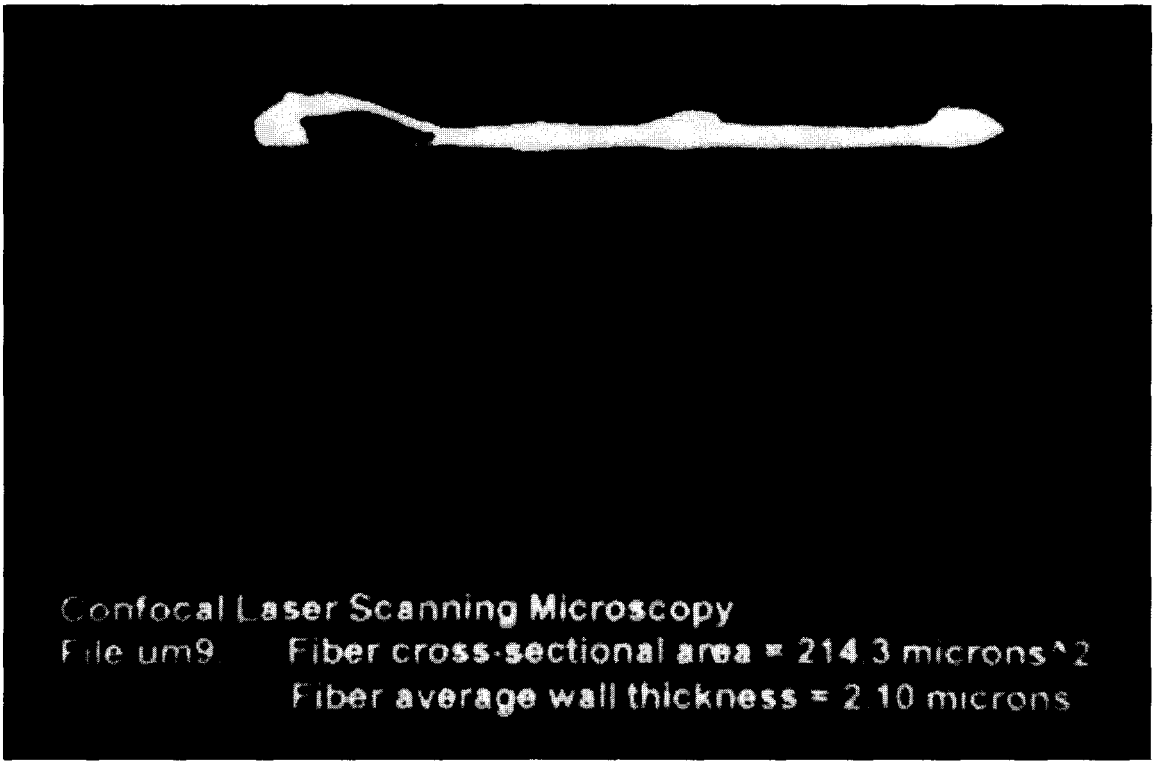

Figure 5—Confocal, laser-scanned photomicrograph of XZ section of an individual, loblolly pine, earlywood tracheid.

mechanisms in small wood specimens. Figure 6 shows an individual, latewood, loblolly pine fiber failing in tension, with failure initiating at and propagating around a bordered pit (Mott and others 1995). Coupling this information with DIC would show local deformations. Digital image correlation, conducted in matrix form, would allow mapping the strains of an individual specimen under known testing conditions. The potential for determining fundamental information about the performance of individual wood components by combining several imaging techniques is phenomenal.

Conclusion

Fundamental knowledge of the mechanical behavior of wood components, whether acting individually or in concert within wood-based composites, is necessary to ensure a high product quality and to engineer next-generation composites that are superior in efficiency and strength to their predecessors. Digital imaging systems are fast becoming a standard research tool that allow the researcher to quantify physical and mechanical properties of component and composite performance. Combining several of the techniques presented in this paper will allow researchers to gather information that is accurate and, until recently, has been unobtainable.

Literature Cited

Chu, T.C.; **Ranson,** W.F.; Sutton, M.A.; Peters, W.H. 1985. Applications of digital image correlation techniques to experimental mechanics. Experimental Mechanics. 25(3): 232-244.

Hamad, W.Y.; **Provan,** J.W. A novel fatigue-testing experimental technique for single wood pulp fibers [in press]. Experimental Mechanics.

Luo, P.F.; Chao, Y.J.; Sutton, M.A.; Peters, W.H. 1993. Accurate measurement of three-dimensional deformations in deformable and rigid bodies using computer vision. Experimental Mechanics. 33(2):123-132.

McMillin, Charles W. 1974. Dynamic torsional unwinding of southern pine tracheids as observed in the scanning electron microscope. Svensk Papperstidning. 9: 3 19-324.

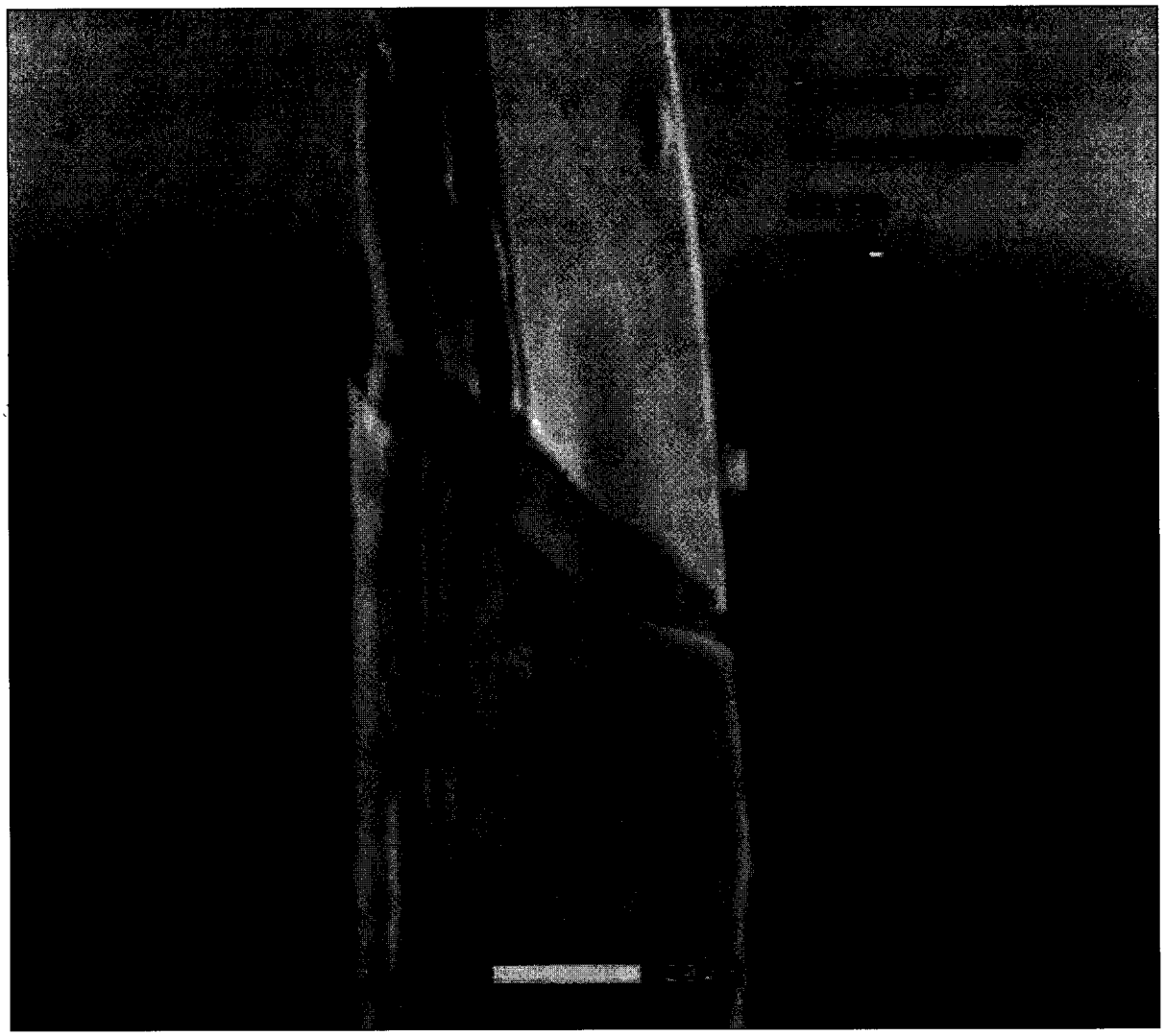

Figure h---Environmental scanning electron microscope image of an individual latewood, loblolly pine fiber subjected to tensile loading.

Mercado, Julius S. 1992. Using digital image analysis to determine the reinforcement of wood fiber polyurethane composites. Houghton, MI: Michigan Technological University. 82 p. M.S. thesis.

Mott, L.; **Shaler,** S.M.; Groom, L.H.; Liang, B.H. 1995. The tensile testing of individual wood fibers using environmental scanning electron microscopy and video image analysis. Tappi. 78(5):143-148.

Page, D.H.; El-Hosseiny, F.; **Winkler,** K.; Lancaster, A.P.S. 1977. Elastic modulus of single wood pulp fibers. Tappi. 60(4): 114-l 17.

Full Field Stress/Strain Analysis: Use of Moiré and TSA for Wood Structural Assemblies

Ronald W. Wolfe, Robert Rowlands, and C.H. Lin

Abstract

Moiré and thermoelastic stress analysis (TSA) methods were compared on the basis of an assessment of the stress distribution in metal plate connectors loaded in axial tension. For the 12.7 mm gauge length considered, the moiré technique had a strain resolution of 1,000 $\mu\epsilon$ without computer enhancement and 200 $\mu\epsilon$ with computer enhancement using digital image analysis and Fourier interpolation. Using the commercial SPATE@ equipment, TSA had a resolution of roughly 145 psi (1 MPa) in steel, corresponding to a strain of 5 $\mu\epsilon$.

Results of these tests show the TSA test equipment to be superior for laboratory testing of metallic materials. For field evaluation of wood structures, however, the moiré method has the potential to be more portable, to be less costly, and to have the same or a superior resolution when enhanced using digital image analysis.

An analysis of metal gusset plates stressed in tension confirm the expected stress distribution characteristics. Stresses are rarely uniformly distributed over the width of the plate. The assumption of a uniform distribution of tooth loads along the length of a plate is reasonable for connections designed with a balance between tooth withdrawal and steel tensile failure. For longer plates prone to steel failure, the plate teeth nearest the joint carry a higher load than teeth closer to the end of the plate.

Introduction

Structural wood components and assemblies have been evolving for over 200 years in the United States to meet the ever-changing demands on available energy and material resources. Over the past 40 years, Americans have seen major changes in the way wood is used in structural applications: plywood has replaced board sheathing, trusses have replaced lumber rafters, and wood l-joists have regained a significant share of the commercial building market that was lost to steel in the early part of this century.

Ronald W. Wolfe is a research engineer, USDA Forest Products Laboratory, One Gifford Pinchot Dr., Madison, WI 53705; Robert Rowlands is a professor of engineering mechanics, University of Wisconsin, Engineering Hall, Madison, WI 53706; and C.H. Lin is a research engineer, Sunoco Products Co., P.O. Box 160, Hartsville, SC 29950.

To compete with other materials in meeting the continuing demands for energy and material resources, the use of improved test and analytical procedures that facilitate the identification of design imbalances must be explored. Tools for performing full-field analyses of stress and strain enable stress concentrations to be identified and the range of stress/strength ratios to be quantified within a given structure. These tools provide the potential for further developments toward optimizing the use of wood fiber resources.

The use of two, full-field, analysis tools for the evaluation of wood-frame truss connections is examined in this paper. Moiré and thermoelastic stress analysis (TSA) methods have been widely used in machine and tool design and to a more limited extent in the development of design guidelines for steel structures and connections. While these tools have been applied to wood and wood-fiber-based materials at the basic research level, they are rarely used in product development or for field evaluation. State-of-the-art developments in image analysis used in conjunction with these tools give them valuable potential for a broad range of applications in wood structures research and development.

Background And Theory

Moiré and TSA methods are convenient tools for the full-field analysis of member stresses. The moiré method is a more mature technology with the advantage of a much broader experience base. Its uses range from high-resolution, laboratory, interferometry techniques to field applications where it is used simply to assess strain concentrations with relatively little concern for stress magnitude.

The TSA method has the advantage of enabling direct/remote assessment of member stresses. Measurements are calibrated on the basis of stress, giving some advantage where the modulus of elasticity varies or is unknown. It does not require any applications of rulings to the structure surface. The primary disadvantage of TSA is the higher equipment cost.

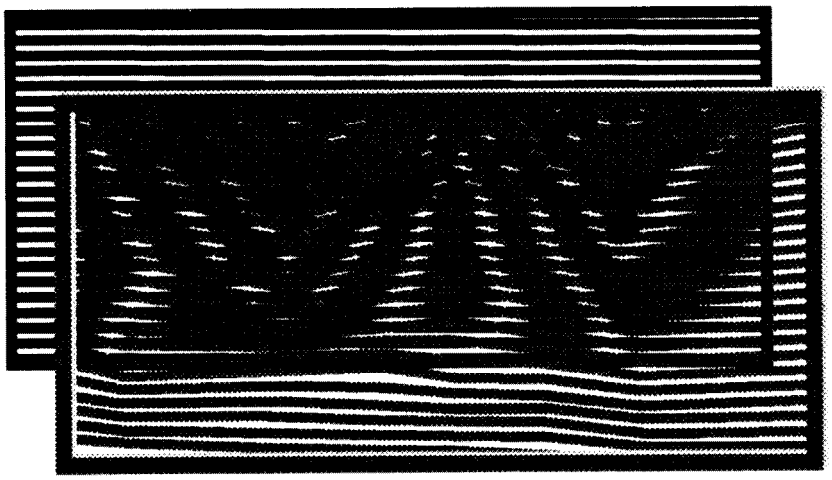

Figure 1-A linear moire line pattern showing that hot interference fringes are generated by grid overlay. The deformed (specimen) grid blocks light passing through the undeformed (analyzer) grid at locations where the accumulated mismatch in the spacing of specimen line intervals equals the analyzer line spacing.

Moiré Fringe Analysis

Full-field strain analysis using moire techniques is a fairly well-established procedure in the field of experimental mechanics. Moire analyses employ optical geometric interference as a tool for assessing strain. While interferometric moire techniques have tended to be confined to laboratory conditions, techniques employing film overlays have expanded its use to less restrictive applications. Optional techniques used to enhance the moire technique include grid vs. line patterns for biaxial vs. uniaxial strain measurement, initial rotational or linear mismatch, digital image analysis to amplify conventional resolution, and fractional fringe and interferometry.

The basic theory of the moire method is easy to understand and to apply. When two, closely spaced, line arrays having similar, but not identical, patterns are superimposed and viewed with transmitted or reflected light, interference fringes are generated where lines from one line array block the light transmitted between the lines of the second array (fig. 1). Any distortion of one (active/specimen) array relative to the other (analyzer) array will result in changes in this fringe pattern that can be used to assess the location as well as the magnitude of surface strain.

Two methods of enhancing the interference patterns are to begin with a slight rotation of the analyzer (fig. 2) and to use a small mismatch in the analyzer array vs. the specimen array. An initial rotational mismatch facilitates the differentiation of tension and compression zones. Initially, the rotation causes an array of fringes oriented at one-half the rotational angle from the strain direction. As the specimen is strained, compression on the specimen will

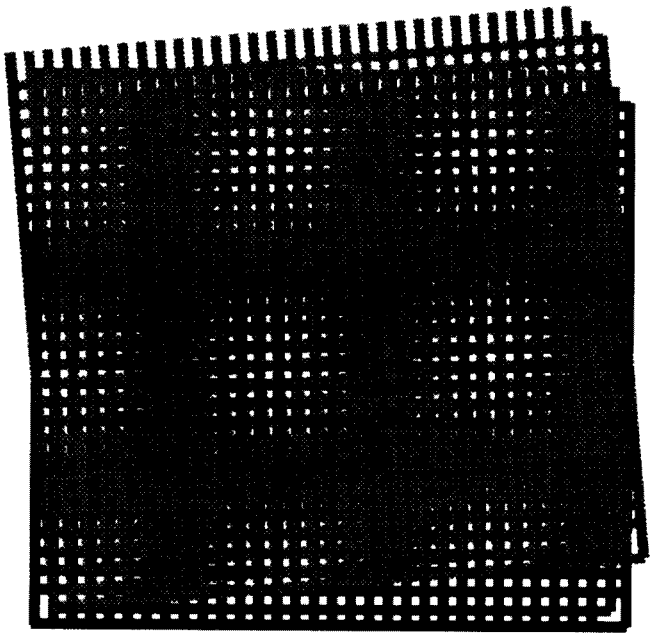

Figure 2-The rotational mismatch of moire, biaxial, grid patterns shows initial interference fringes with no distortion of the specimen.

cause a decrease in the rotational angle of the fringes while tension will cause an increase in fringe rotation. A small, linear mismatch results in an initial fringe pattern running perpendicular to the principal strain direction. Tension will cause a gain in the number of fringes, and compression will cause a reduction in the number of fringes per unit length.

By recording the progression of the moire image using a charge-coupled device (CCD) camera, the variation in shades of gray between fringes, quantified using an image processor, may be characterized as a periodic function using Fourier series to interpolate strains across the entire strain field. This technique can be used to divide a visible fringe into four or five quantifiable increments, thus increasing strain resolution.

A 2,000 line-per-inch moire film used to assess strain over a gauge length of 12.7 mm [the approximate length of tooth slots in metal plate connectors (MPC's)] will show only a fringe when displacement in that gauge length reaches 0.0254 mm, which is close to the yield point of steel. Being able to detect one-third of the fringe displacement within 12.7 mm will give the strain in the range of design load.

In addition to its use for evaluating stresses in MPC's, the use of the moire method for evaluating the performance of composites is being contemplated. The use of the moire method is not confined to uniaxial strain analysis. By using a moire grid, one can evaluate biaxial strains, including shear strain. This technique has been documented by Post (1965).

Thermoelastic Stress Analysis

Belgen (1967) first documented the use of noncontact TSA. In 1982, a British company, Ometron Ltd., began marketing the first commercial TSA system, which they called SPATE' [Stress Pattern Analysis (by measurement of) Thermal Emission].

$$\Delta T = -K_m T \Delta (\sigma_x + \sigma_y + \sigma_z)$$

The theoretical basis for thermoelastic stress analysis lies in the first and second laws of thermodynamics. The most commonly referenced derivation for the relationship between temperature change and material stress relates only to elastic deformation (Rauch and Rowlands 1993). Under cyclic loading, this derivation can be simplified to a direct linear relation (Eq. 1) that estimates the change in temperature as a function of the change in stress times a thermoelastic material constant and ambient temperature.

The thermoelastic material constant is inversely related to material density and specific heat, and directly related to the coefficient of thermal expansion. If the material is orthotropic, the coefficient of thermal expansion is likely to vary with the principal axis of the material, causing the thermoelastic material constant to be different in each direction.

A limiting factor in the application of TSA techniques is the required control on the loading frequency, which must be acceptable for adiabatic material response; that is, the thermodynamic process must be reversible, requiring a balance between the thermal and the mechanical energy. For most metals, this requires a frequency above 2 Hz. For materials of decreasing thermal conductivity, however, the necessary frequency for adiabaticity increases. For example, wood requires 18 Hz or more.

SPATE provides digital output, which, when color calibrated, gives a graphic interpretation of how stresses vary over the stressed field. While an observer cannot pick up the resolution of the color thermograph when it is copied in black and white, figure 3 gives some idea of the kind of output obtained from SPATE. In this figure, the lighter strands are heavily stressed over the region of the butt joint. Above the third row of strands, there is evidence of nonsymmetric load as stresses are larger for areas on the right side of the plate.

Numerical techniques were used to smooth the digitized output and give stress distribution plots as shown in figures 4 through 7. A slight compressive stress shown near the end of the plots in figures 4 and 5 was caused when the row of teeth farthest from the joint began to peel out of the wood, bending the plate and compressing the surface.

An analysis of the digitized data suggests a fairly uniform distribution to the various rows of teeth for a 7.6 by 12.7 cm plate designed with a balance between tooth-holding and steel tensile stresses (fig. 5). As would be expected, stress in the steel strands is greatest between the first and second rows of teeth. The drop in stress is due to the load being transferred by the teeth into the wood. The drop in surface stress is roughly the same across each double row of teeth, suggesting that the load transferred to the wood is the same for each double set.

The TSA analysis of a 7.6 by 25.4 cm plate (fig. 8) at 4.45 kN shows that the drop in axial stress is not uniform over the length of the plate. This analysis suggests that for longer

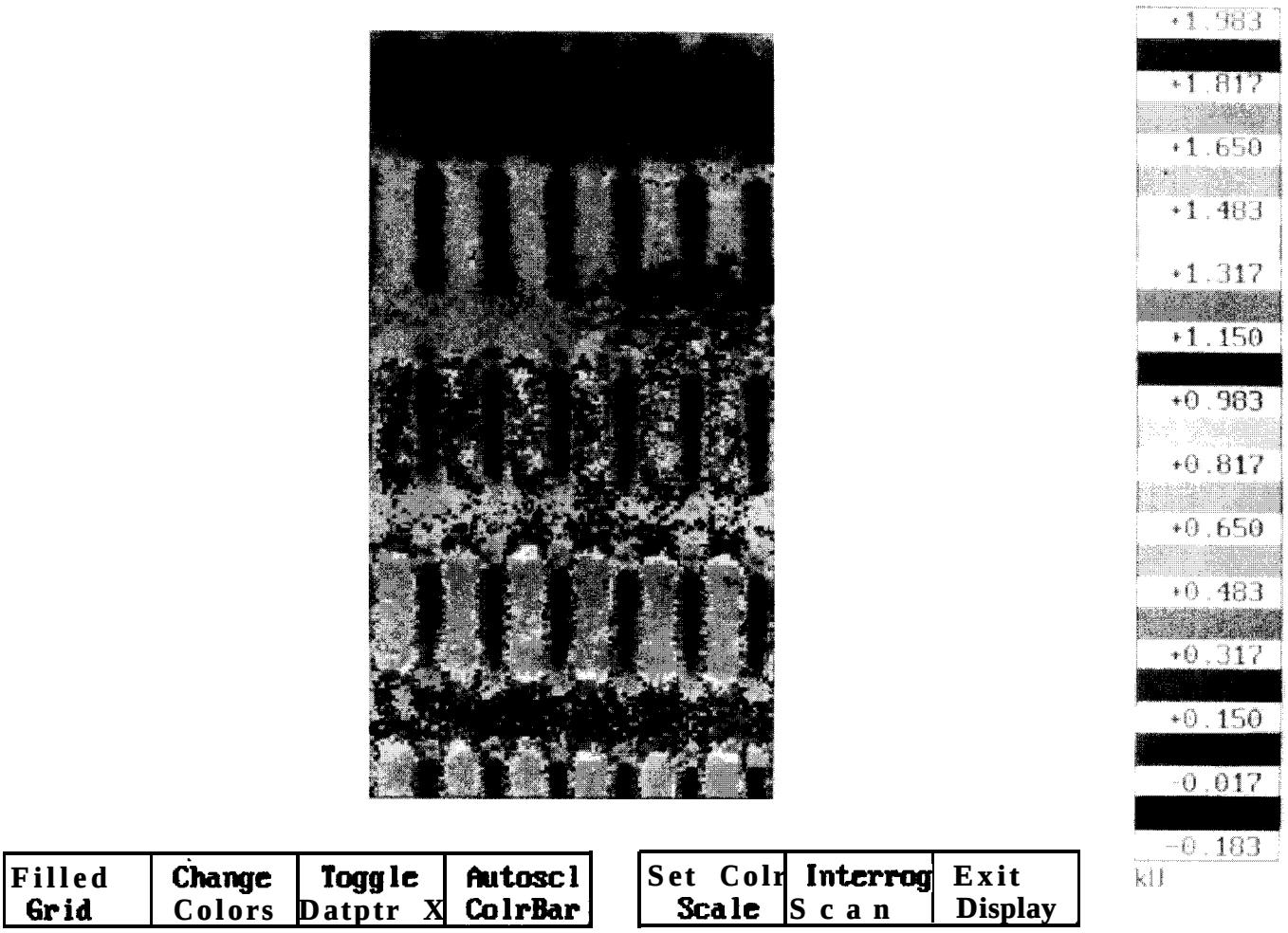

Figure 3-A black-and-white copy of a color thermogram showing the distribution and variation of stress in a metal connector plate stressed in axial tension.

plates, the tooth load decreases from the joint to the ends of the plate.

When looking at a more confined region, along steel strands between rows of teeth, the effects of stress concentration at the root of the strands can be seen (fig. 6). Axial stress appears to decrease toward the middle of the strands. Shear stress, however, increases toward the middle of the strand, where the failure occurs in a steel plate under axial stress.

While the popular use of TSA is for stress evaluation in metal parts, it can be applied directly to wood. Figure 9 shows a piece of wood containing a knot stressed by compression. This application has not received much attention, but as this technology evolves, it has potential for use in lumber grading, product development, and structural evaluations. as well as in basic research.

Conclusion

Both the moir and TSA methods have potential for future developments that will make use of growing computer technology. While moiré technology is more mature than TSA and has been applied to many different problems, developments in the area of digital image correlation can enhance its value as a precision tool for full-field strain analysis.

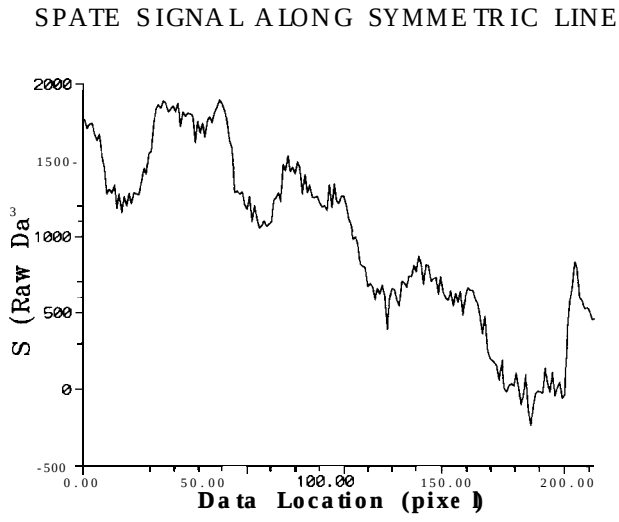

Figure &The measured distribution of stress in plate strands and cross bars over half the length of a 7.6 by 12.7 cm plate extending from the joint to the end of the plate.

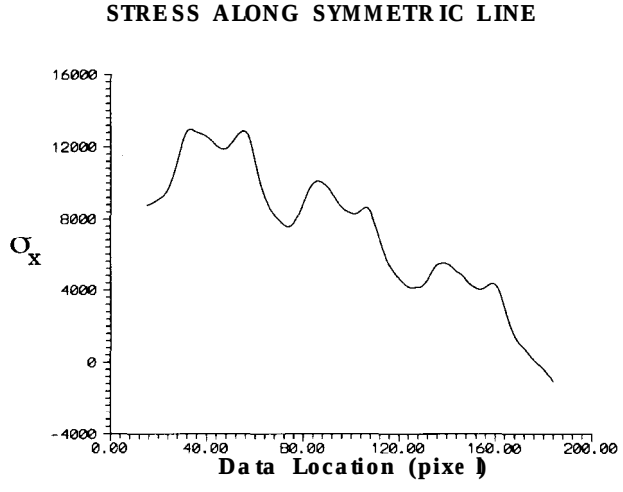

Figure 5-A smoothed, axial stress distribution plot over half the length of the plate.

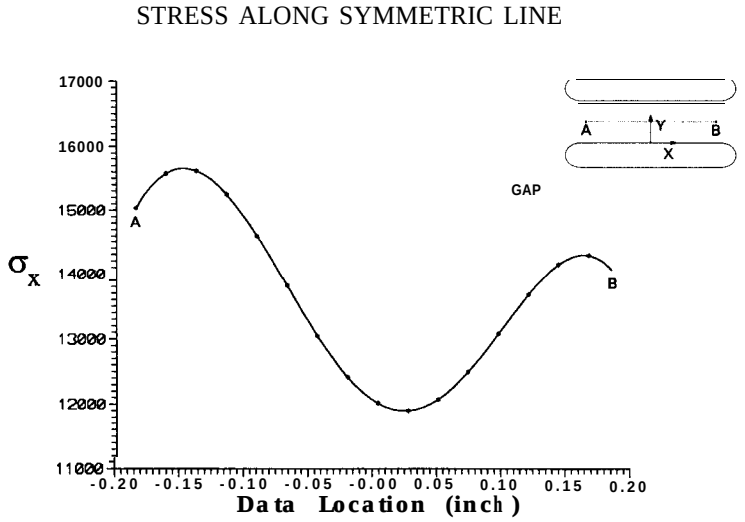

Figure 6—The distribution of axial stress along the length of a single strand shows that the highest axial stresses were near the roots of the strand due to stress concentrations.

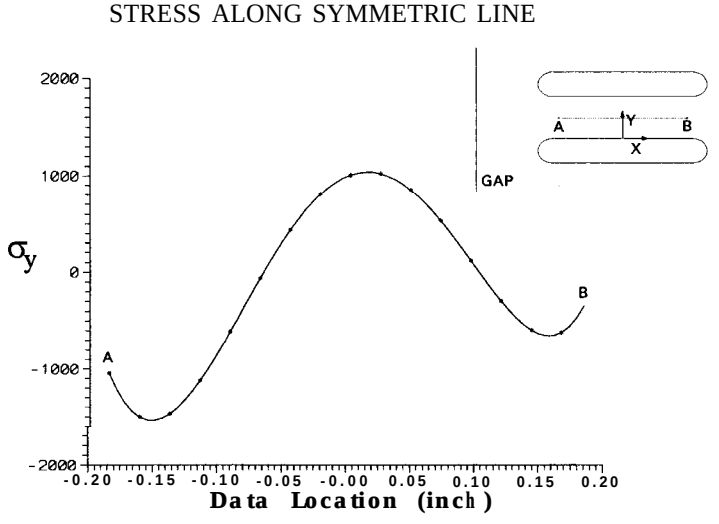

Figure 7-The variation of the average transverse stress along the strand length.

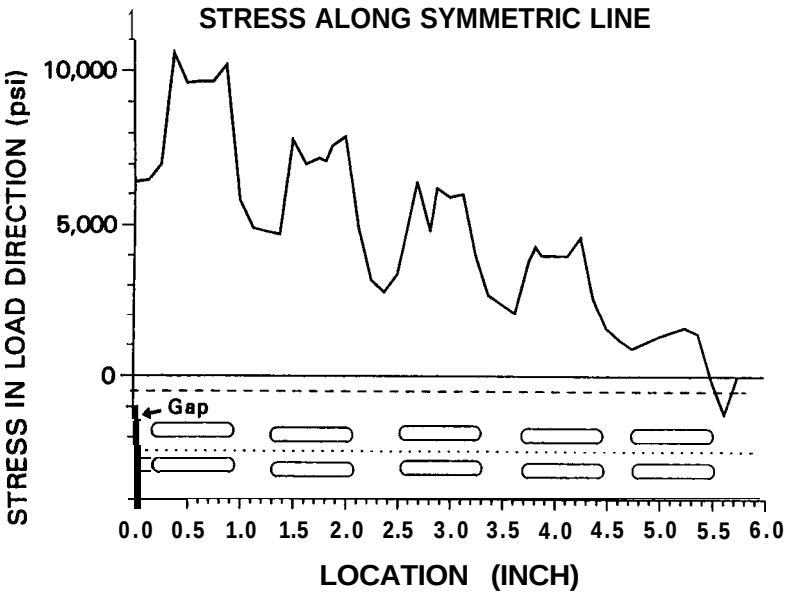

Figure 8—The distribution of axial stresses over half the length of a 7.6 by 25.4 cm plate.

This study demonstrated the first known application of TSA to wood. While it suggests some serious limitations, it shows TSA's potential for future applications in lumber or veneer stress grading.

The application of both the moire and TSA methods to MPC joints has shown variations in stress along the length of the plate and at stress concentration points. Either of these techniques would be useful in optimizing connector plate configurations.

Advantages of the moire method over the TSA method include cost, portability, and the ability to easily take a reading at any load. The ease of using moire film overlays, along with development of CCD cameras and digital image correlation techniques, provides the potential for taking full-field strain measurements in the field. By permanently attaching a moire pattern to highly stressed members in a structure, periodic checks can be made to assess changes in the state of stress. Availability of a new portable interferometric camera should greatly increase the effectiveness and versatility of moire applications to wood.

The primary advantages of TSA are its direct measurement of member stress and its resolution. The TSA measurements have a resolution comparable to that of strain gauges with the advantages that nothing has to be attached to the specimen and that the measurements are directly correlated to stress.

Companies concerned with the development of products whose performance is sensitive to stress concentrations may choose to conduct studies using the moire method on their own, or contract with a private testing lab or university such as the University of Wisconsin, to take advantage of the capabilities of TSA.

Acknowledgments

This project was funded through a USDA Competitive Grant (Project # 9202563) awarded to establish a verification data base for plated connection analytical models. We are grateful to S.H. (Ted) Lin for his assistance in performing some of the SPATE analyses included in this project.

Literature Cited

Belgen, M.H. 1967. Structural stress measurements with an infrared radiometer. Instrument Society of America Transcripts. 6:49-53.

Post, D. 1965. The moir grid analyzer method for strain analysis. Experimental Mechanics. 5(11): 368-377.

Rauch, B.J.; Rowlands, R.E. 1993. Thermoelastic stress analysis. In: Kohayashi, AS., ed. Handbook on experimental mechanics. [Place of publication unknown]: VCH Publishers. Chapter 14.

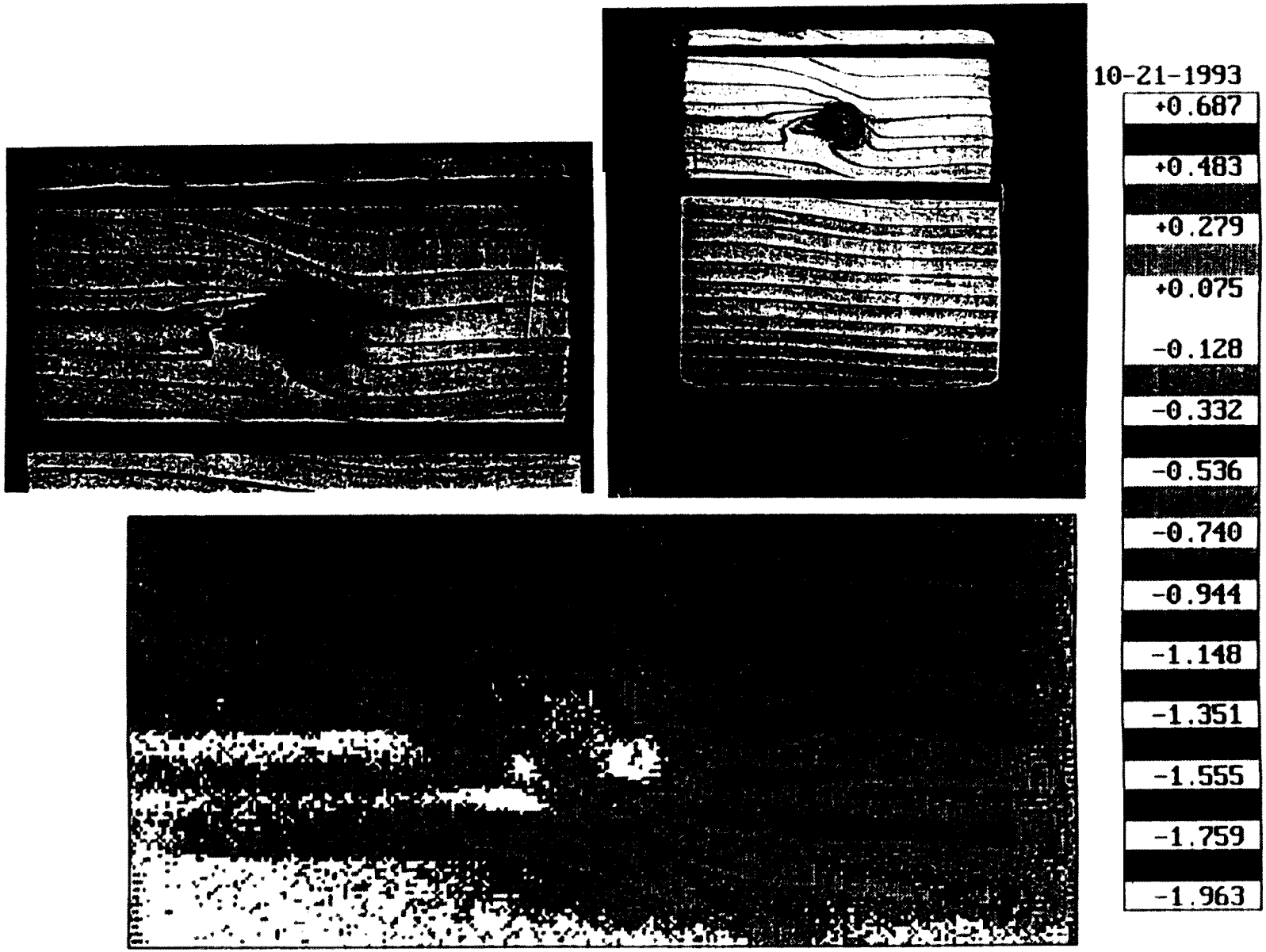

Figure 9—A TSA thermogram under axial compresision.

Characterizing the Wood Fiber/Polymer Interface

T.G. Rials, M.P. Wolcott, and D.J. Gardner

Abstract

The last several years have seen an extensive research effort addressing a relatively novel composite system composed of wood fibers and thermoplastic polymers. In large part, this research has helped to define the problems associated with the development of this type of composite and to identify a significant void in our current knowledge. For example, one major consideration for this composite is the limited compatibility that commonly exists between these two dissimilar materials. Consequently, poor adhesion between the phases is commonplace leading to poor stress transfer from the plastic matrix to the stronger wood fiber. In short, an inadequate fiber/polymer interface significantly limits mechanical property development. Not surprisingly, because of the experimental challenges presented by the small fiber size, very few studies have focused on the direct evaluation of the interfacial characteristics of the wood fiber/polymer composite system. Recently, research in a number of laboratories has demonstrated the usefulness of several analytical techniques that are available to investigate this important component. The advantages and limitations of several of the more promising micro-mechanical methods under development are discussed, including: (1) the fragmentation test, (2) the fiber pull-out test, (3) the micro-debond test, and (4) dynamic mechanical analysis. In addition, examples of their application to lignocellulosic, fiber-based composites will be described in order to highlight the value of the fundamental information that is derived by defining the physico-chemical parameters controlling the quality of the fiber/matrix interface.

Introduction

The use of wood fibers as a reinforcing phase in thermoplastic polymers has been identified as an attractive alternative use for low-value timber species and recycled fibers. These renewable fibers offer such favorable characteristics as high strength and toughness, low weight, and reduced abrasion of compounding equipment. There are, however, several challenges that need to be overcome before significant advances in wood fiber reinforced polymers (WFRP's) can be realized. One of the more prevalent issues is the relatively widespread incompatibility that has been observed between wood fibers and the synthetic thermoplastic polymers that are logical matrix candidates (Kokta 1988). The inherent chemical dissimilarities (e.g., hydrophilic vs. hydrophobic) between the two phases of the composite generally result in poor adhesion. As a consequence, stress transfer from the matrix to the fiber is inadequate, and the performance properties of the resulting composite suffer.

Given the significant contribution of the fiber/matrix interface to composite properties, it is not surprising that a substantial research effort has focused on improving the compatibility of wood fibers with various thermoplastics like polyethylene, polypropylene, and polystyrene. While this research has typically involved relatively well-defined and well-understood chemical modifications of the fiber's surface (or the plastic matrix), evaluating the effect of individual treatments on interfacial strength and quality has presented a tremendous challenge. Early investigations relied primarily on evaluating the effect of fiber content on composite properties, thereby defining a "fiber efficiency factor" (Dalvag and others 1985). It became obvious that processing variables, such as fiber damage and orientation, greatly influenced the interpretation of the data in terms of the quality of the fiber/matrix interface. An alternative approach that has recently been reported is to evaluate the effect of surface modifications on adhesion using a conventional peel test (Kolosick and others 1992), or a modified pull-out experiment with small wooden dowels embedded in a thermoplastic matrix (Sanadi and others 1992). These approaches have effectively eliminated the previously described complications and have demonstrated considerable value as approaches for the rapid and convenient evaluation of different surface-modifying treatments. However, it is virtually impossible to extrapolate this data to the fiber composite system due to the complications introduced by the morphological and macroscopic features of the wood substrate. In addition, the information provided by these experimental methodologies fail to provide the fundamental information on the fiber/matrix interface that is needed to adequately model this hybrid composite material.

In response to the shortcomings of previous experimental approaches designed to study the strength of the wood fiber/polymer interface, several methods have been adopted

T.G. Rials is a research physical scientist, USDA Forest Service, Southern Research Station, 2500 Shreveport Hwy., Pineville, LA 71360; M.P. Wolcott and D.J. Gardner are assistant professors. Division of Forestry, West Virginia University, 206-B Percival Hall, Morgantown, WV 26506-6125.

and refined from outside the wood science arena. Four of the more promising analytical techniques that have been applied to this novel composite system include: (1) the fiber fragmentation test, (2) the fiber pull-out test, (3) the micro-debond test, and (4) dynamic mechanical analysis. In this discussion, particular emphasis will be given to the type of information that can be derived from these different micro-mechanical methods, as well as to the limitations presented by each approach.

Background

The quality of the fiber/matrix interface is not an entirely new issue because it is relevant to virtually any type of composite system including polymer blends, copolymers, and filled polymers. The significance of the interface in any composite material originates from the different chemical and physical environments that are present at the boundary between the different phases (Lipatov and others 1980).

Strong interaction between two materials can dramatically alter the properties of the interfacial region by restricting the mobility of the local polymer molecules. As a result, the interface region is typically characterized by a property gradient between the two pure phases (fig. 1). It is important to recognize that strong adhesion between phases can also negatively affect the properties of the composite material. Consequently, it is important to define and understand interfacial, structure-property relationships to optimize the composite's performance.

The contribution of the fiber/matrix interface to the composite's performance does seem to be more critical in wood fiber/thermoplastic composites than in conventional wood composites bonded with thermosetting resins. Although many considerations, such as wettability, are common to both types of composite systems, the interface between wood fibers and thermosetting resins has been studied more from a microscopic level than the interface in wood fibers/thermoplastic composites. The relatively low

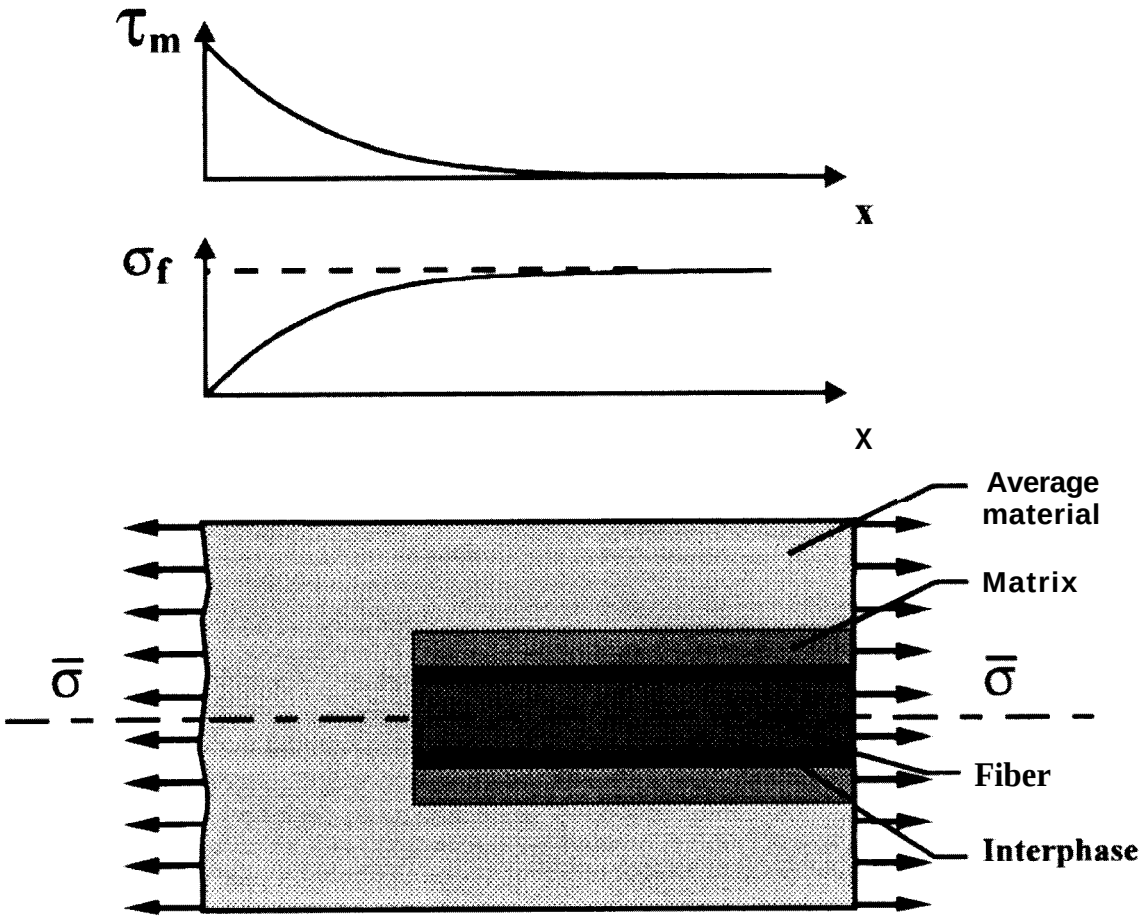

Figure 1-A schematic illustration of a composite model with the contribution of the fiber/matrix interface

molecular weight and chemical reactivity of the resin mean that adhesive bonding can be achieved through penetration and mechanical attachment, and possible chemical reaction, between the resin and the wood fiber. By contrast, the thermoplastic system is characterized by high molecular weight and limited chemical reactivity, suggesting that the adhesion between phases is dominated by secondary interactions (i.e., hydrogen bonding). Because these interactions are of relatively low energy, the fiber/matrix interface may only consist of several molecular layers, presenting a significant analytical challenge. For this reason, it is imperative to evaluate the wood fiber/ thermoplastic polymer interaction under conditions that realistically simulate the actual environment of the composite. Recent developments in micro-mechanical test methods are beginning to make a real contribution to this experimental problem and are providing the fundamental information needed to understand and model the contribution of the fiber/matrix interface to the ultimate properties of WFRP composites.

Analytical Techniques

It is worth emphasizing from the outset of this discussion that, while each of the micro-mechanical tests presents its own challenges and limitations (table 1), there are several cautions that are common to all of them. First, given the small size of the fiber and the sample as a whole, handling and sample preparation represent the most significant challenges to be overcome in the application of these techniques. Second, given the small interfacial area being investigated, the presence of any voids or defects at the interface will effectively invalidate any results. This can be a

Table l-Summary of the advantages and disadvantages of fiber/polymer interfacial test methods

Test Method	Advantages	Disadvantages
Fiber Fragmentation (Critical Fiber Length)	Direct measure of fiber/polymer interface strength	Requires ductile matrix polymer
	Stress optical analysis	Requires information on in-situ fiber strength
Fiber Pull-out	Indirect measure of fiber/ polymer interface strength	Sample preparation (with fibers) is difficult
	Information on interfacial failure mechanism	Tapered fiber end complicates data analysis
Micro-debond	Eliminates problem from tapered fiber ends	Fiber failure may be dominant for strong interface
	Fiber strength information not required	
	Relatively fast and simple	
Dynamic Mechanical Analysis	Links molecular structure to properties	No direct measure of interfacial strength
	Provides a measure of interfacial volume	

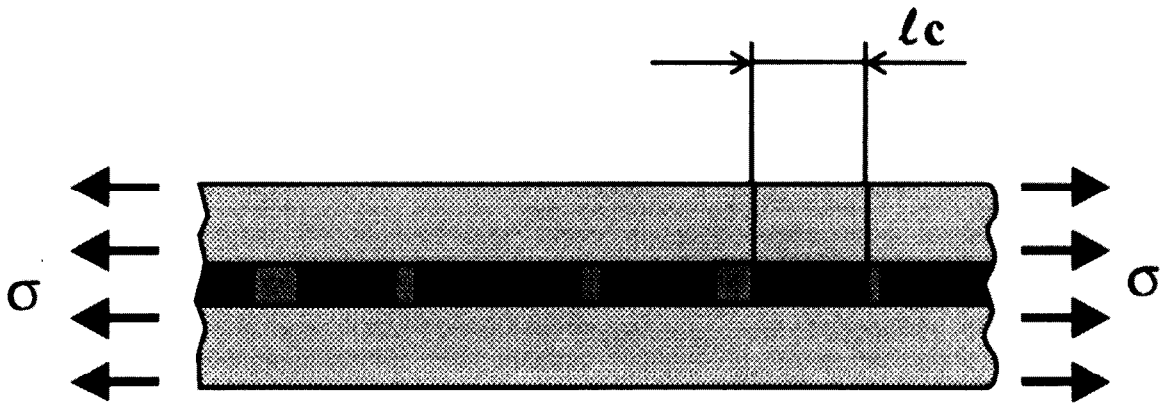

Figure 2-A schematic illustration of the fiber fragmentation test showing applied stress, , and critical fiber length, 1,.

tremendous problem when using a reactive polymer system where the evolution of volatile reaction products often occurs (e.g., phenolic resins and polyurethanes). Finally, it is important to recognize that frictional stress transfer, rather than adhesive stress transfer, can be important and can complicate analyses and comparisons between the various methods. In short, attention to detail at all stages of experimentation is critical to generating valid data.

Fiber Fragmentation Test-The fiber fragmentation (Drzal 1985), or critical fiber length test, involves embedding a single fiber in a polymer matrix and stressing the sample in the direction of the fiber's longitudinal axis (fig. 2). As the tensile load increases, the fiber will fracture, decreasing the segment size until a critical length, l_c, is reached, which is too short to transfer the stress needed to break the fiber. The critical fiber length can be related to the shear strength (τ_c) at the fiber/polymer interface by:

$$\tau_c = \frac{\sigma_f d}{2 l_c} \qquad (1)$$

where

$_f$ = the fiber tensile strength and d the fiber diameter.

Additional information on interfacial strength and stress transfer efficiency can be obtained for translucent, birefringent, matrix materials by viewing the deformation process with polarized light microscopy to enhance the image. This allows the observation of the stress field in the matrix polymer, providing some insight into adhesion mechanisms. Figure 3 is a stress optical micrograph of a wood fiber embedded in polyethylene and shows the concentration of stress around a natural fiber defect, illustrating the utility of this approach. Note the stress concentration in the matrix near the fiber ends. Samples with poor interfacial properties would show little variation in the stress field along the fiber length.

Samples can be produced by some relatively simple approaches including dispersing a few fibers in a polymer solution and casting a film. In order to eliminate solvent effects, the fibers can be placed between two polymer films and compression molded. Individual samples can then be isolated by punching test specimens with appropriate fiber orientation from the polymer sheet. Perhaps the greatest restriction on the widespread use of the fiber fragmentation test is the requirement of relatively ductile matrices that are capable of strain levels above 3 percent. However, alternative test designs are under investigation to minimize this problem (Lee and Holguin 1990). Promising results have been reported using this test procedure for wood fiber composites of polyethylene (Tai and others 1992).

Fiber Pull-Out Test-The fiber pull-out test (Wang and others 1988) involves embedding fibers to different depths in the plastic matrix of interest as illustrated in figure 4 and provides a critical fiber length similar to the fragmentation test described above. Alternatively, individual fibers can be embedded in small buttons of the polymer, and the force required to extract the fiber can then be determined (Lawrence 1972). This experiment is attractive because it can also provide information on the interfacial failure mechanism. Although the exact form of the relationship depends on the type of failure that is observed for the system, the interfacial debonding shear strength (τ_d) for the fracture process can be obtained as follows:

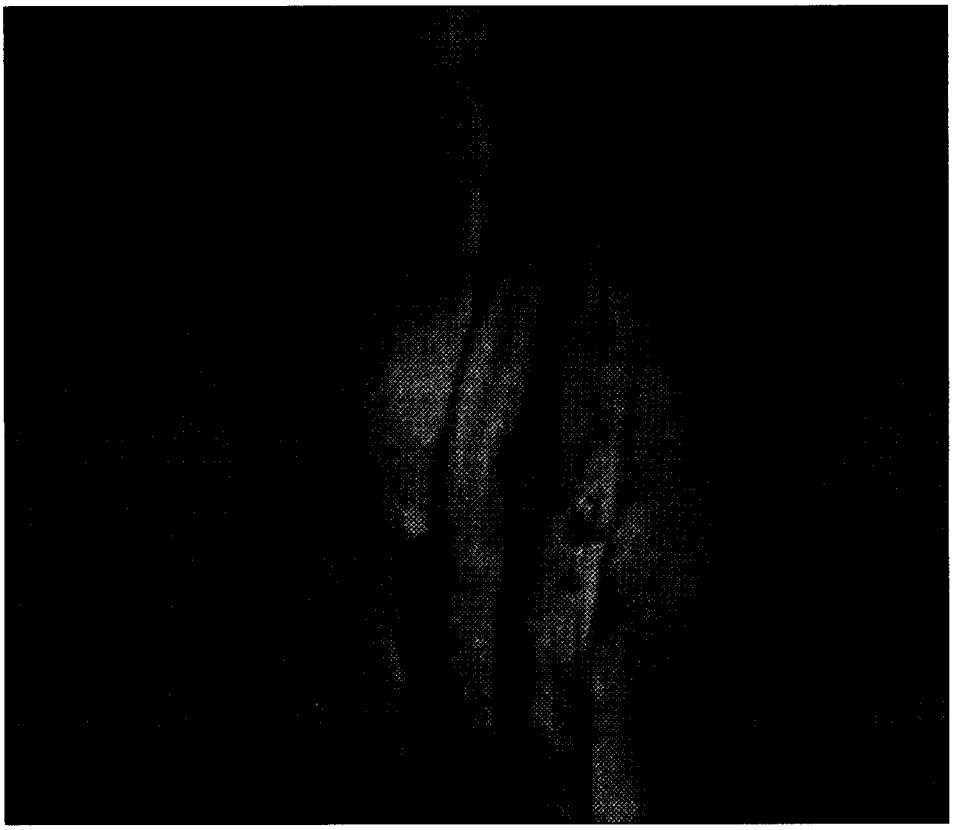

Figure 3-An optical micrograph showing stress in a wood fiber embedded in polyethylene.

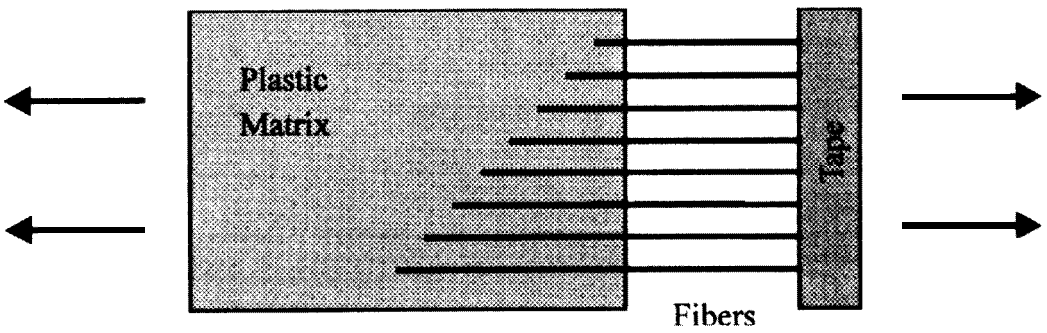

Figure 4—A schematic diagram of the critical fiber length pull-out test

$$\tau_d = n\sqrt{\frac{E_f G_i}{r}} \qquad (2)$$

where

E_f = the fiber modulus,
G_i = the work of fracture of the interphase,
r = the fiber radius, and
n = a constant related to the properties of the two components.

This test has been used to evaluate the effects of different surface chemical modifications on the adhesion of polyethylene to wooden dowels (Sanadi and others 1992). Unfortunately, it has not been applied extensively to wood fiber/polymer systems due in part to the difficulties associated with accurately controlling the embedded length of the fiber.

In addition, the characteristic tapered ends of lignocellulosic fibers greatly complicate the experiment and interpretation of the data. Regardless, this approach holds considerable promise because it is much more tolerant of the polymer matrix properties and is sensitive to the type of failure.

Micro-Debond Test-The micro-debond test (Gaur and Miller 1989) or micro-droplet test, is similar to the fiber pull-out test in its approach and the type of information it provides. The preparation of the sample involves first solvent casting a thin film of the polymer matrix and cutting a rectangle that is slit in the middle (similar to a pair of trousers). The polymer "trouser" film is then hung on a horizontal fiber mounted on a support and melted to form a droplet. A small vise (fig. 5) is mounted on the testing machine to grip the droplet, and the force required to detach the polymer from the fiber is measured. The fiber/matrix interfacial shear strength (τ_{max}) is estimated from the relation:

$$\tau_{max} = \frac{P_{max}}{\pi D l} \qquad (3)$$

where

P_{max} is the maximum load, D is the fiber diameter, and l is the embedded fiber length.

The micro-debond test offers several important advantages over the previously discussed methods including the fact that the fiber strength or fiber strength/embedded length relationships are not a consideration in this approach. Also, the shear strength distribution can be assumed to be uniform over a wide range of the embedded fiber aspect ratio. The most critical factor in the successful use of this experiment is control of the droplet size and of the interfacial area. If the area is too large, then fiber failure prior to debonding can become dominant. These problems have largely been overcome by Liu and others (1995). Their investigations on wood fiber/polystyrene composites indicate that the micro-debond test provides a relatively simple and rapid method for evaluating interfacial properties. Figure 6 shows typical force-displacement results for polystyrene on rayon, cotton, and wood fibers. From these experiments, a linear relationship between the surface energy of the fiber and the interfacial shear strength was established.

Dynamic Mechanical Analysis-Dynamic mechanical analysis (Rosen 1982) provides a sharp contrast to the previously discussed analytical approaches in that it is a nondestructive test. In this experiment, the sample is subjected to a small sinusoidal strain that allows the storage and loss components of the complex modulus to be resolved (fig. 7). By monitoring the variation in the storage

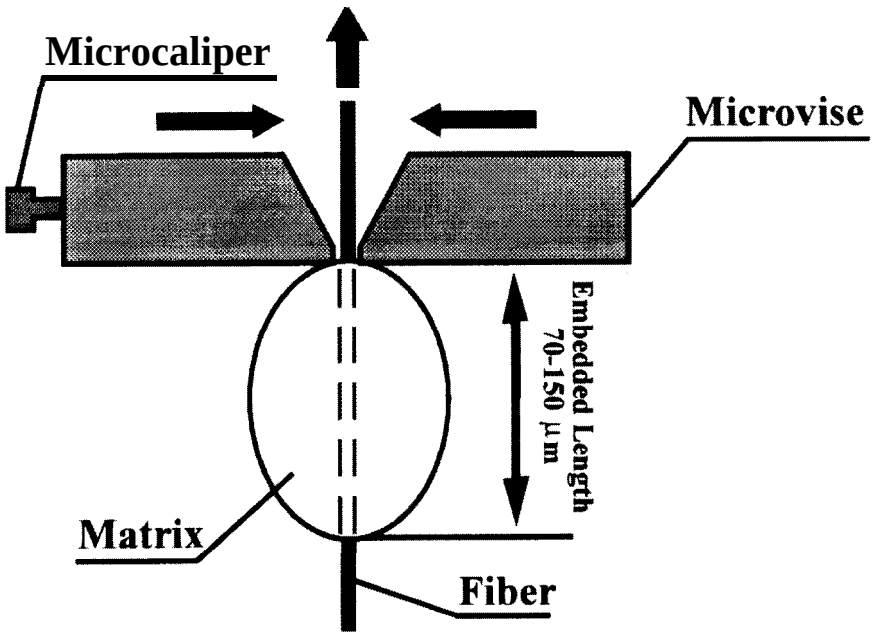

Figure 5-A schematic illustration of the micro-debond test geometry.

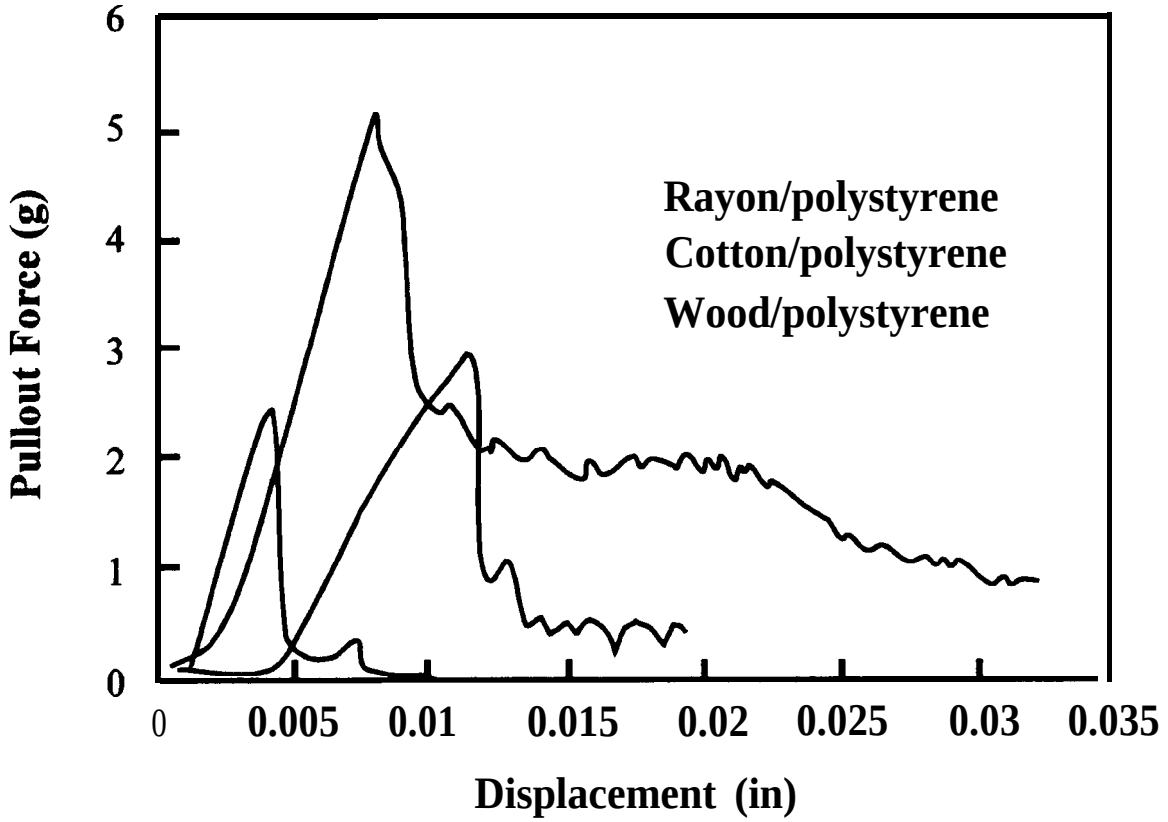

Figure 6—Typical results from the micro-debond test for polystyrene on wood, cotton, and rayon fibers.

and loss modulus over a wide range of temperatures and frequencies, the viscoelastic spectrum of a material can be generated. The interest in dynamic mechanical analysis lies in the sensitivity of this method to molecular motion and the relaxation properties of the composite material. Given that strong interactions between the fiber and polymer can substantially alter the mobility of polymer chains at the interface, this technique can provide insight into the mechanics of interfacial interactions and the relative volume of the interface or interphase. Consequently, this test method provides complementary information that is necessary to completely characterize the properties of WFRP's.

The dynamic mechanical data presented in figure 8 clearly illustrates the value of this nondestructive procedure (Nassar 1994). Polyurethane composites were prepared with thermomechanical pulp (TMP) fiber, mechanically regenerated newsprint fiber, and acetylated TMP fiber (the chemical reactivity decreases in that order), and a synthetic polyol. The intense tan peak at approximately -40 °C, common to all of the spectra, represents the glass transition of the purely synthetic urethane phase. The unmodified TMP fiber, which is considerably more reactive in this system, exhibits a dramatically lower peak height as well as a high temperature shoulder from about -25" to 10 "C. This suggests that a high chain density interphase is established more effectively with this fiber than with either of the other fiber composite systems. The influence of this fiber/polymer interphase on the material properties of the composite results in a considerably higher storage modulus (E') at higher temperatures. It should be clear from this example that dynamic mechanical analysis provides a critical link between the molecular and phase structure and the mechanical properties of wood fiber/polymer composites.

Conclusion

The ultimate properties of wood fiber/thermoplastic polymer composites are determined not only by the

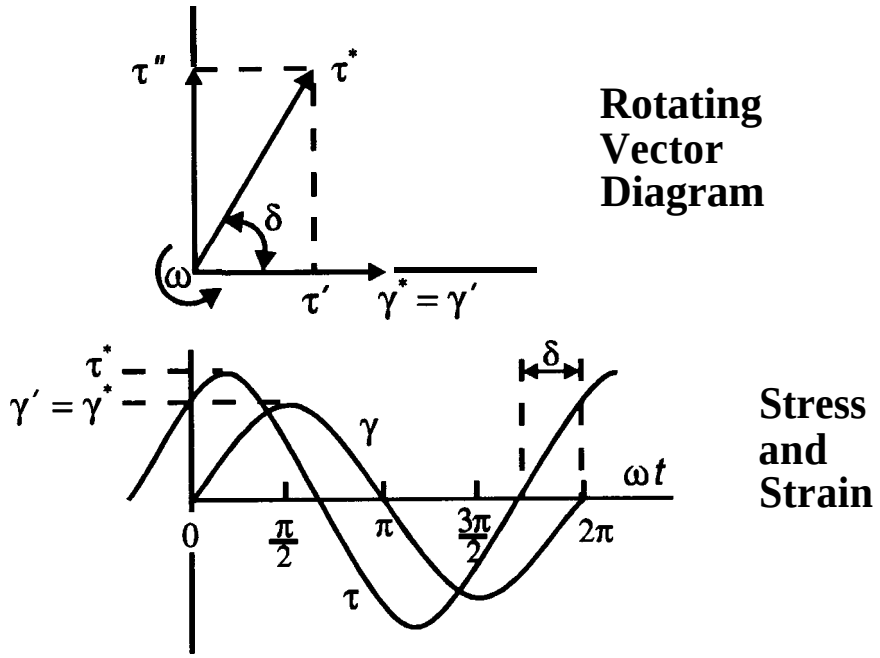

$G^* = G' + iG''$ (complex modulus)

$G' = \tau'/\gamma'$ (storage modulus)

$G'' = \tau''/\gamma'$ (loss modulus)

$\tan\delta = \tau'/\tau'' = G'/G''$ (loss tangent)

Figure 7 -Parameters provided by dynamic mechanical analysis.

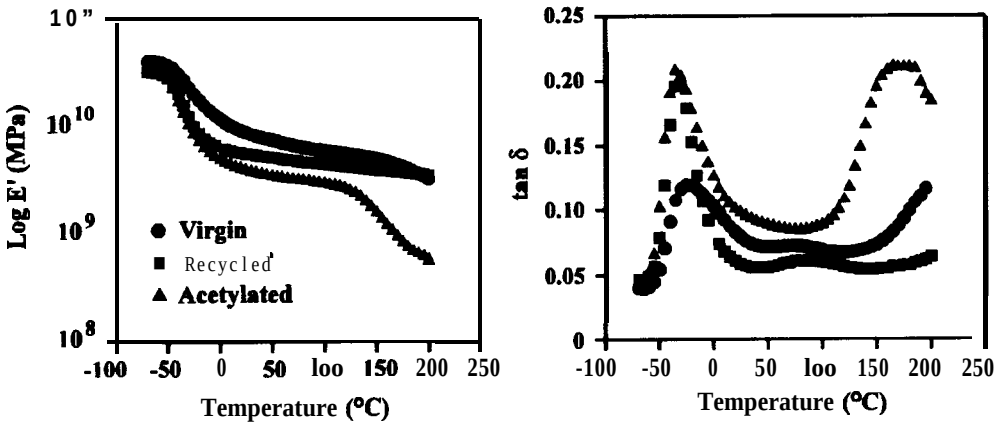

Figure X-Dynamic mechanical spectra (log E' and tan 6) of polyurethane composites prepared with thermomechanical pulp fiber, acetylated thermomechanical pulp fiber, and recycled newsprint fiber.

properties of the fiber and the plastic, but also by the characteristics of the fiber/matrix interface. As such, it is imperative that reliable experimental techniques be available for the determination of interfacial properties under conditions that realistically simulate the stress distributions of the use environment. Although considerable progress has been made, it is apparent that no single technique can satisfy this requirement at present. Rather, an integrated approach is required that carefully considers the characteristics of the fiber/polymer system under investigation in selecting the appropriate micro-mechanical test method.

Literature Cited

Dalvag, H.; Klason, C.; Stromvall, H.E. 1985. The efficiency of cellulosic fillers in common thermoplastics: Filling with processing aids and coupling agents. International Journal of Polymeric Materials. 11: 9-38.

Drzal, L.T.; Rich, M.J.; Koenig, M.F. 1985. Adhesion of graphite fibers to epoxy matrices. III. The effect of hygrothermal exposure. Journal of Adhesion. 18: 49-72.

Gaur, U.; Miller, B. 1989. Microbond method for determination of the shear strength of a fiber/resin interface: Evaluation of experimental parameters. Composites Science and Technology. 34: 35-51.

Kokta, B.V. 1988. Use of wood fibers in thermoplastic composites Polymer News. 13(11): 331-333.

Kolosick, P.C.; Myers, G.E.; Koutsky, J.A. 1992. Polypropylene crystallization on maleated polypropylene-treated wood surfaces: Effects on interfacial adhesion in wood/polypropylene composites. In: Rowell, R.M.; Laufenberg, T.L.; Rowell, J.K. eds., Materials interactions relevant to recycling of wood-based materials: Materials Research Society Symposium Proceedings; April 27-29, 1992; San Francisco, CA. Pittsburgh, PA: Materials Research Society. 266: 137-154

Lawrence, P. 1972. Some theoretical considerations of fibre pull-out from an elastic matrix. Journal of Material Science. 7(1): l-6.

Lee, S.M.; Holguin, S. 1990. A new single fiber/resin interface test for highly cross-linked resin systems. Journal of Adhesion. 31: 91-101.

Lipatov, Y.S.; Rosovitsky, V.F.; Babich, B.V.; Kvitka, N.A. 1980. On shift and resolution of relaxation maxima in two-phase polymeric systems. Journal of Applied Polymer Science. 25(4):1029-1037.

Liu, P.F.; Gardner, D.J.; Wolcott, M.P.; Rials, T.G. 1995. Characterization of the interface between cellulosic fibers and a thermoplastic matrix. Composite Interfaces. 2(6): 419-432.

Nassar, J.M. 1994. Production and analysis of wood fiber polyurethane composites. Morgantown, WV: West Virginia University. M.S. thesis.

Rosen, S.L. 1982. Fundamental principles of polymeric materials. 2d ed. New York, NY: Wiley-Interscience. Chapter 18.

Sanadi, A.R.; Rowell, R.M.; Young, R.A. 1992. Estimation of fiber-matrix interfacial shear strengths in lignocellulosic-thermoplastic composites. In: Rowell, R.M.; Laufenberg, T.L.; Rowell, J.K., cds., Materials interactions relevant to recycling of wood-based materials: Materials Research Society Symposium Proceedings; 1992 April 27-29; San Francisco, CA. Pittsburgh, PA: Materials Research Society. 266: 81-92.

Tai, W.C.; Quarles, S.L.; Rials, T.G. 1992. The effect of compatibilizers on interfacial bonding in lignocellulosic fiber/polyethylene composites. In: Kennedy, J.F.; Phillips, G.O.; Williams, P.A., eds. Cellulosics: chemical, biochemical and material aspects, part 3. New York: Ellis Horwood. Chapter 74, 507-5 12.

Wang, Y.; Backer, S.; Li, V.C. 1988. A special technique for determining the critical lengths of fiber pull-out from a cement matrix. Journal of Material Science. 23: 842-844.

Appendix

Table l-Summary of presentation discussing strain measurement using traditional devices (Speaker: Joe Loferski)

Category	Equipment	cost	Advantages	Limitations	Possible applications
Extensometers	LVDT	$500	Accurate, high resolution	Heavy, bulky, involves electronics	Measuring relatively displacements
	Digital Dial Gauges	$450	Accurate, easy to use	Relatively expensive, heavy, bulky	Measuring dimensions, deflections
	Mechanical Dial	$50	Accurate, east to use, inexpensive	Limited resolution, cumbersome	Measuring dimensions, deflections
Strain Transducers					
(a) User-built	LVDT's, Dial Gauges, Strain Gauges	Variable	Developed for specific uses, low cost, reuseable, large or small length	Development time, reliability and accuracy questionable	Measuring strains, distances, dimensions, and displacements
(a) Commercial	Variety of special test devices	High	Development is already done, accuracy guaranteed, industrial support	Expensive	Measuring strains, distances, dimensions, and displacements
Electrical Strain Gauges	Strain gauges, clamps, wire, adhesive, electronics, solder	$5-$125 (size dependent)	Accurate, reliable, industry support	Cost, gauge length, patience	Bonds directly to specimen for accurate strain measurements

Table 2-Summary of presentation discussing the digital image correlation technique in experimental stress analysis(Speaker: Audrey Zink)

Category	Equipment	cost	Advantages	Limitations	Possible applications
Image Acquisition	CCD camera	$500-$2,000	Non-contacting	Portability limited	Unlimited, any material, any load type, any environmental conditions
	Illuminators	$500-$1,000	Necessary for consistent lighting	Must be unchanging	Provide uniform lighting
	Image Capture Board	$1,500-$3,000	Allows digital acquisition of images	Must be coupled w/computer and CCD camera	Image acquisition and subsequent storage
Image Correlation	Computer and Software LVDTs, Dial Gauges, Strain Gauges	$2,000-$20,000	Full-field and point-to-point strain measurement, non-contact	Limited by computer power, memory	Measure strain distributions, concentrations, elastic constants, dimensional changes

Table 3a—Summary of presentation discussing the application of new imaging technologies to experimental mechanics (Speaker: Laurence Mott)

Category	Equipment	cost	Advantages	Limitations	Possible applications
Light microscopes	Transmitted/Reflected/ Incident Light Microscope	$6,000 $30,000	Inexpensive, low-maintenance, easy to use; very high resolution	No contrast, limited surface information	Morphological measurements (when connected to CCD camera); general observations; used as polariscope for ohotoelastic observations
	Confocal Scanning Laser Microscope (CSLM)	$80,000- $250,000	Allows 3D observations and recon-structions (rotation about all axes); highest resolution of various confocal microscopes	Expensive, specimen often requires staining to flouresce; image acquisi-tion time may be slow; no real time image building	3-D morphological measurements of various x-, y-, and z- planes; micromechanics (esp. fracture process); fiber and paper sections
	Deconvolution-type confocal microscope	$20,000- $30,000	Inexpensive 3D imaging; given micro-scope, only stage and software needed; out-of-plane blur removed with deconvolution software	Limited sectioning available; computationally intensive	Microbiology; limited use in micromechanics
	NIPKOW Disk type confocal microscope	$20,000- $30,000	3D imaging of materials; morphometric measuring in x-, y-, and z-directions	Limited sectioning available; difficulty in obtaining cross-sectional areas	Microbiology; limited use in micromechanics
	Direct Video Microscope	$30,000- $60.000	Large focal field, versatile, high magnification possible	Expensive	General observations; good for large, specimens
Electron Microscopes	Scanning Electron Microscopes (SEM)	$60,000- $170,000	Very high magnification, good surface detail	High-vacuum environment, specimens (non-conductive) need coating in a brittle medium (gold)	Morphology of individual fibers; study of failure mechanisms in composites, adhesive/ coating distribution on wood components
	Environmental SEM (ESEM)	$150,000- $250,000	No conductive coating needed, water can exist in liquid state (due to higher pressures); dynamic testing	Expensive; maintenance Intensive, generally requiring agreement of approximately $10,000 year	Observation of failure mechanisms of small specimens (individual fibers, adhesion) during dynamic testing; fiber hydration
Digital Image Processing	Digital Image Enhancement	$200- 54,000	Allows user to increase visual contrast within a digital image	If not careful, may alter original digital image; time intensive	Used to show areas of high contrast; useful in studying fracture mechanisms and resin distributions
	Morphometric Measurements	$1,500- 56,000	Measurements can be made quickly using macros; helps reduce bias	Requires some training, and access to digital images; macros generally specific for certain sample	Excellent for determining length, width, and thickness distributions within a sample
	Digital Image Correlation	$0- $3,000	Allows remote sensing of non-contact strains; allows for measurement of active and passive strains	Need capability to acquire successive digital images during testing; code needs to be written or modified by user	Determination of local stiffnesses within a solid or composite specimen
Image Acquisition	CCD camera	$1,500- $30,000	Allows images to be stored digitally for morphological measurements or contrast enhancement; flexible images, quantitative imaging	Resolution of image proportional to cost of camera and frame grabber; best CCD camera cannot match the quality of standard analog camera	Necessary for digital assessment of morphological characteristics, and for acquisition of digital images (archival and comparison purposes)
	Tube cameras	$1,500- $15,000	Very high resolution and spectral sensitivity	Analog images need framegrabbers to be used quantitatively; supporting resolution framegrabbers tend to be expensive, physically less robust	High magnification and high resolution microscopy (e.g. CSLM); microbiological sciences
	Frame Grabber	$800- $10,000	Necessary hardware which interfaces CCD camera with processor	Resolution of image proportional to cost of camera and frame grabber; resolution of frame grabber should approximate that of the CCD camera	Necessary for digital assessment of morphological characteristics, and for acquisition of digital images (archival and comparison ourposes)

Table 3b—Supplemental information for presentation on applying new imaging technologies to experimental technologies (Speaker: Laurence Mott)

Technique	Setup cost	Technical considerations
ESEM microtensile stage	ESEM facilities can be purchased on an hourly basis. Few facilities have the microtensile stage assembly which costs about $7,000. Need to manufacture own tensile grips. A LaB6 filament can also be purchased for about $1,000. The filament increases contrast and base quality.	Crosshead movement typically 1-100 microns/second. Maximum load around 100 lbs. Fast (near TV) scan rate can be used when testing large solids. Condenser lens can be adjusted to avoid burning the sample over time. Images can be used for digital image correlation. Possible to condense water droplets on sample.
Basic CCD imaging systems	Cameras of medium resolution cost approximately $1,000. RGB high resolution monitor costs $1,000~. Framegrabber cost = $1 ,OOO+. A computer w/sufficient memory essential. 640x640 image = 300k. Lenses cost anywhere from $500+. Extension tubes can be used to convert the system into a video microscope.	Matching chip and lens size is important. Using a larger lens size than chip is preferable. Smaller chip size leads to better resolution. Chip size from 5 to 25 mm. Good signal to noise ratio of 52dB+. Higher resolution = lower light sensitivity. Color cameras may have 1, 2, or 3 chips. Signal can be extracted from these individually.
Alternative Scanning Micrographs	None	A 600 dip scanner can digitize a high resolution micrograph. The image can then be used in the same fashion as a digitally acquired image. Copy centers generally offer a high resolution scanning service.
Free software	None	Kohroe is one of the most powerful digital image processing packages available. This UNIX-based system is available thru ftp from the University of New Mexico. For Macintosh computers, NIH is one of the best digital imaging packages available free on the public domain.

Table 4—Summary of presentation discussing full-field stress analysis using moiré and thermo-elastic stress analysis (Speaker: Ron Wolfe)

Category	Equipment	cost	Advantages	Limitations	Possible applications
Full-Field Stress Analysis	Moire Master Grid	$900	Portability	Strain measurement	Lab or field evaluation of stress around connections
	Photo Developing Equipment	$1,000	Photographic prints adhered to test surface or direct exposure of photo sensitive emulsion	Requires knowledge of material MOE for stress analysis	Stress patterns in engineered composites used as webs or shear diagrams
	CCD camera	$2,000	Improved resolution; no need to convert analog to digital		
Full-Field Stress Analysis	S.P.A.T.E.	$120,000	Resolution comparable to strain gauges; direct evaluation of material stresses	Expensive, not easily used in field	Connections, quality control for engineered components

Table 5—Summary of presentation discussing the characterization of the interface in wood fiber/polymer composites (Speaker: Mike Wolcott)

Category	Equipment	cost	Advantages	Limitations	Possible applications
Thermo-Dynamic Properties	Dynamic Mechanical Analyzer	$70,000-$120,000	Links molecular structure and physical behavior; provides thermal relations of mechanical properties	Small samples; difficult to incorporate moisture control; best for solid systems	Viscoelastic characterization: determination of glass transition temperature; determination of polymer morphology: composite structure
Mechanical Properties	Miniature Materials Tester	$18,000	Produces load-elonation traces of small specimens, thus providing mechanical properties; small enough to fit under conventional microscope for material observation	Small specimen size; low load capacity; monotonic loading	Stress optical analysis; determination of of mechanical properties of small specimens

Groom, Leslie I-I.; Zink, Audrey G. 1998. Techniques in experimental mechanics applicable to forest products research-Proceedings of a Plenary Session at the Forest Products Society Annual Meeting; 1994 June 26-29; Portland, ME: Gen. Tech. Rep. SO-125 Asheville, NC: U.S. Department of Agriculture, Forest Service, Southern Research Station. 45 p.

Presents opening remarks and presentations of five speakers from a plenary session on techniques in experimental mechanics presented at the FPS Annual Meeting in Portland, ME on June 26-29, 1994. Information presented in this report is aimed at forest products researchers and the forest products industry.

Keywords: Strain measurement, extensometers, transducers, digital image correlation, strain mapping, enviromnental scanning electron microscope, confocal scanning laser microscope, imaging, moire, SPATE@, metal plate connectors, interface, micro-debond, fragmentation, critital fiber length.

The Forest Service, U.S. Department of Agriculture, is dedicated to the principle of multiple use management of the Nation's forest resources for sustained yields of wood, water, forage, wildlife, and recreation. Through forestry research, cooperation with the States and private forest owners, and management of the National Forests and National Grasslands, it strives-as directed by Congress-to provide increasingly greater service to a growing Nation.